Computational and Structural Biotechnology Journal 21 (2023) 1169–1188

Contents lists available at ScienceDirect

Computational and Structural Biotechnology Journal

journal homepage: www.elsevier.com/locate/csbj

Review

Structured population balances to support microalgae-based processes: Review of the state-of-art and perspectives analysis

Alessandro Usai [a,b], Constantinos Theodoropoulos [a,b], Fabrizio Di Caprio [c], Pietro Altimari [c], Giacomo Cao [d,e,f], Alessandro Concas [d,e,*]

[a] Department of Chemical Engineering, University of Manchester, M13 9PL Manchester, United Kingdom
[b] Biochemical and Bioprocess Engineering Group, University of Manchester, M13 9PL Manchester, United Kingdom
[c] Department of Chemistry, University Sapienza of Rome, Piazzale Aldo Moro 5, Rome, Italy
[d] Department of Mechanical, Chemical and Materials Engineering, University of Cagliari, Piazza d'Armi, 09123 Cagliari, Italy
[e] Interdepartmental Center of Environmental Science and Engineering (CINSA), University of Cagliari, Via San Giorgio 12, 09124 Cagliari, Italy
[f] Center for Advanced Studies, Research and Development in Sardinia (CRS4), Loc. Piscina Manna, Building 1, 09050 Pula, CA, Italy

ARTICLE INFO

Article history:
Received 8 November 2022
Received in revised form 28 January 2023
Accepted 29 January 2023
Available online 31 January 2023

Keywords:
Population balance equations
Microalgae biorefineries
Mathematical modelling
Downstream processes
Optimization

ABSTRACT

Design and optimization of microalgae processes have traditionally relied on the application of unsegregated mathematical models, thus neglecting the impact of cell-to-cell heterogeneity. However, there is experimental evidence that the latter one, including but not limited to variation in mass/size, internal composition and cell cycle phase, can play a crucial role in both cultivation and downstream processes. Population balance equations (PBEs) represent a powerful approach to develop mathematical models describing the effect of cell-to-cell heterogeneity. In this work, the potential of PBEs for the analysis and design of microalgae processes are discussed. A detailed review of PBE applications to microalgae cultivation, harvesting and disruption is reported. The review is largely focused on the application of the univariate size/mass structured PBE, where the size/mass is the only internal variable used to identify the cell state. Nonetheless, the need, addressed by few studies, for additional or alternative internal variables to identify the cell cycle phase and/or provide information about the internal composition is discussed. Through the review, the limitations of previous studies are described, and areas are identified where the development of more reliable PBE models, driven by the increasing availability of single-cell experimental data, could support the understanding and purposeful exploitation of the mechanisms determining cell-to-cell heterogeneity.

Contents

* Corresponding author at: Department of Mechanical, Chemical and Materials Engineering, University of Cagliari, Piazza d'Armi, 09123 Cagliari, Italy.
E-mail address: alessandro.concas@unica.it (A. Concas).

https://doi.org/10.1016/j.csbj.2023.01.042

Nomenclature

$\boldsymbol{b}(\boldsymbol{m}, \boldsymbol{m}')$	Daughter distribution function, (ng^{-1}).
$\boldsymbol{B}(m)$	Born rate of cells of mass m, (ng^{-1} mm^{-3} hr-1).
$\boldsymbol{B_a}$	Born rate due to aggregation, (ng^{-1} mm^{-3} hr^{-1}).
$\boldsymbol{B_b}$	Born rate due to aggregates breakage, (ng^{-1} mm^{-3} hr^{-1}).
$\boldsymbol{C_j}$	Concentration of j^{th} nutrient in the medium ($j = 1 \Rightarrow NO_3^-; j = 2 \Rightarrow H_2PO_4^-$), (g m^{-3}).
C_{O2}	Dissolved O_2 concentration in the growth medium, (g m^{-3}).
$\boldsymbol{C_{O2}^{max}}$	Maximum O_2 concentration tolerated by algae medium, (g m^{-3}).
$\boldsymbol{d}$	Equivalent diameter of the cell, (μm).
$\boldsymbol{d_c}$	Critical diameter at which the cell is committed to divide, (μm).
$\boldsymbol{D}$	Disappearance rate of cells of mass m, (ng^{-1} mm^{-3} hr^{-1}).
$\boldsymbol{D_a}$	Disappearance rate due to aggregation, (ng^{-1} mm^{-3} hr^{-1}).
$\boldsymbol{D_b}$	Disappearance rate due to aggregates breakage, (ng^{-1} mm^{-3} hr^{-1}).
$\boldsymbol{Dil}$	Dilution rate, (hr^{-1}).
$\boldsymbol{E_{D,z}}$	Axial dispersion coefficient, (m^2 s^{-1}).
$\boldsymbol{f}(\boldsymbol{m})$	Probability density that a cell of mass m divides when approaching critical mass, (/).
$\boldsymbol{h_i}$	Distribution in terms of frequency for the mass class I for unit mass, (ng^{-1}).
$\boldsymbol{H}(\boldsymbol{I_{av}})$	Heavyside function accounting that cell division occurs only in the dark, (/).
$\boldsymbol{I_{av}}$	Average photosynthetically active radiation within the culture, (μE m^{-2} hr^{-1}).
$\boldsymbol{I_{dir}}$	Directed photosynthetically active radiation within the culture, (μE m^{-2} hr^{-1}).
$\boldsymbol{I_0}$	Incident photosynthetically active radiation, (μE m^{-2} hr^{-1}).
$\boldsymbol{K_I}$ or $\boldsymbol{K_{I1}}$	Half saturation constant in the light-dependent term of the growth kinetics, (μE m^{-2} hr^{-1}).
$\boldsymbol{K_{I2}}$	Inhibition constant in the light-dependent term of the growth kinetics, (μE m^{-2} hr^{-1}).
$\boldsymbol{m}$	Single cell mass, (ng).
$\boldsymbol{m_c}$	Critical mass at which the cell is committed to divide, (ng).
$\boldsymbol{m'}$	Mass of the generic mother cell, (ng).
N or n	Number of cells, (/).
$\boldsymbol{p}$	Position in the cell cycle, (/).
$\boldsymbol{p_i}(\boldsymbol{m}, \boldsymbol{m}')$	Partitioning function for the case of division into *i* daughter cells, (ng^{-1}).
$\boldsymbol{r}$	Vector of space coordinates, (m).
$\boldsymbol{R}$	Radius of the cylindrical photobioreactors, (m).
$\boldsymbol{t}$	Time, (min).
$\boldsymbol{v}$	Single cell volume, (μm^3).
$\boldsymbol{v_{t,s}}$	Terminal velocity, (m s^{-1}).
$\boldsymbol{V}$	Photobioreactor volume, (m^3).
$\boldsymbol{V_{Cells}^T}$	Total volume of cells, (μm^3).
$\boldsymbol{X}$	Biomass concentration, (g m^{-3}).
$\boldsymbol{y_{X/j}}$	Ratio of weight of dry biomass produced to weight of j^{th} nutrient consumed, (/).

Greek letters

$\boldsymbol{\alpha_i}$	Parameter of the Hill-Ng distribution for the case of division into *i* cells, (/).
$\boldsymbol{\beta}(\boldsymbol{\alpha_i}, \boldsymbol{\delta_i})$	Beta function for the case of division into i daughter cells, (/).
$\boldsymbol{\beta_b}$	Breakage kernel, (s^{-1}).
$\boldsymbol{\beta_a}$	Aggregation kernel, (m^3 s^{-1}).
$\boldsymbol{\Gamma}$	Division intensity function, (hr^{-1}).
$\boldsymbol{\delta_i}$	Parameter of the Hill-Ng distribution for the case of division into *i* cells, (/).
$\boldsymbol{\zeta}$	Vector of internal coordinates, (various).
$\boldsymbol{\vartheta}(\boldsymbol{m}, \boldsymbol{m'})$	Self-similar daughter distribution function, (/).
$\boldsymbol{\Theta_i}$	Probability of forming a number of daughter cells equal to (i) per mitotic event, (/).
$\boldsymbol{\lambda_i}$	Distribution in terms of frequency for the mass class i for unit mass, (ng^{-1}).
$\boldsymbol{\mu_{av}}$	Average growth rate, (hr^{-1}).
$\boldsymbol{\mu_{max}}$	Maximum specific rate of single cell growth, ($ng^{1/3}$ hr^{-1}).
$\boldsymbol{\mu_c}$	Mass loss rate of single cell, (hr^{-1}).
$\boldsymbol{\nu_d}$	Single cell division rate, (hr^{-1}).
$\boldsymbol{\nu_m}$	Time rate of change of cell mass m, (ng hr^{-1}).
$\boldsymbol{\nu_p}$	Rate of progression in the cycle, (hr^{-1}).
$\boldsymbol{\varrho}$	Specific weight of cells, (g m^{-3}).
$\boldsymbol{\varrho_f}$	Specific weight of fluid, (g m^{-3}).
$\boldsymbol{\sigma_c}$	Standard deviation of the division probability density function, (ng).
$\boldsymbol{\tau_a}$	Optical extinction coefficient for biomass, (m^2 g^{-1}).
$\boldsymbol{\Phi}$	Filtration coefficient, (/).
$\boldsymbol{\psi}$	Density distribution function of the cell population, (ng^{-1} mm^{-3}).
ω	Angle of incidence of light, (rad).

Superscripts

$\boldsymbol{0}$	Initial conditions, (/).
$\boldsymbol{exp}$	Experimental value,
$\boldsymbol{f}$	Final conditions, (/).

Subscripts

$\boldsymbol{av}$	Average value, (/).
$\boldsymbol{i}$	Number of daughter cells or generic counter, (/).
$\boldsymbol{j}$	Number of nutrients or generic counter, (/).
$\boldsymbol{stat}$	Steady state value, (/).

1. Introduction

Microalgae represent a promising renewable feedstock for the production of several consumer goods ranging from functional food to biofuels, nutraceuticals, bioplastics, pharmaceuticals and feed. The typical configuration of a microalgae-based technology roughly involves four main operating steps: cultivation, harvesting, extraction of target compounds and eventual further refining (Fig. 1). Each of these operations may be carried out by different methods, and more than one valuable products might be obtained. The main process inputs consist of CO_2, water, mineral salts and light to drive the photosynthesis that permits microalgae growing and energy to operate reactors and equipment.

When compared to conventional land crops, microalgae show higher growth rates that result in the need for less land for their cultivation. Microalgae can be cultivated even in saltwater, non-arable lands, and through processes integrated with CO_2 capture from flue gases and wastewater remediation [1].

In light of the above, there is a growing demand for microalgae systems in fields of application that range from food/feed production to the energy [2]. Nevertheless, so far, microalgae-based technology has been viably applied at the industrial scale only for producing high-value end-products such as nutraceuticals and superfoods. However, when aiming to obtain low-value products, such as biofuels or bioplastics, that are typically produced on a massive scale, microalgae technologies are still not widespread due to technical constraints that undermine its economic viability. Accordingly, the implementation of this technology at the industrial production scale requires the optimization of the different unit steps of the process, i.e., cultivation, harvesting and lipid extraction, as well as the abatement of their related costs.

In particular, the scale-up of cultivation systems undoubtedly needs significant improvements. To this aim, suitable process engineering techniques relying on the use of mathematical models capable of predicting the system behavior when changing the operating conditions could be used. Several mathematical models have been proposed in the literature in the last decade to describe microalgae growth under different conditions [3]. Most of them quantitatively describe the evolution of biomass concentration as a function of light density, nutrient availability (CO_2, N, P) and

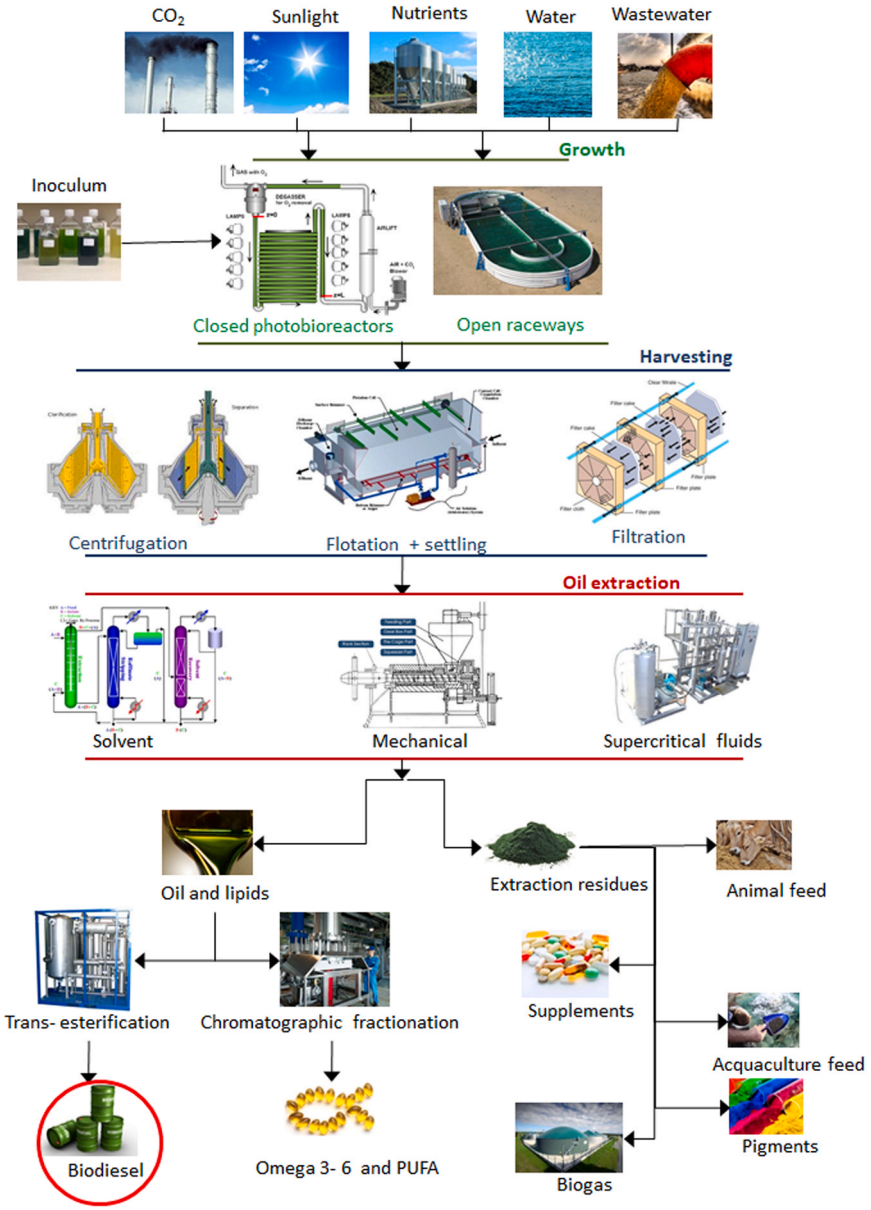

Fig. 1. Proof of concept scheme of a generic microalgae-based bio-refinery.

photobioreactors operating mode [2,4,5]. Several models were focused on the description of the influence of hydrodynamic regime on light availability for microalgae [6,7], while others were able to evaluate lipid production under nitrogen starvation [8–14]. Moreover, models describing the co-production of lipids and carbohyrdates for a biorefinery microalgal technology implementation have also been developed [13a].

Also, in the context of CFDs models, PBMs have a crucial role in describing the bubble size distribution in the gas phase. They provide a more accurate tool to evaluate break-up and coalescence of bubbles in the photobioreactor, which can be important when the specific-area of the gas-liquid interface needs to be accurately evaluated as related to mass transfer phenomena. On the other hand, the bubbles size and distribution could play also a role in light transfer, hydrodynamics, and potentially heat transfer [15].

Though the number, reliability and complexity of mathematical models being proposed are still growing, most assume that individual cells constituting the microalgae population have the same growth rate, biochemical composition and metabolism. It is however widely recognized that microalgae populations consist of cells having different size, morphology, biochemical composition and age, even within a pure monoculture [16–18]. Such heterogeneity may strongly influence the behavior of the cultures. For instance, *Nannocholorpsis oculata* shows a diameter varying between 1.5 and 3.8 μm, corresponding to a variability of the cell volume of about 16 times [19,20]. Relevant cell-to-cell variations have been experimentally determined even for other parameters as the specific growth rate (till 2.4 folds) and for intracellular TAG accumulation under N-starvation till about 400 folds (Table 1).

The accurate evaluation of cell size distribution can provide suitable information to control and optimize the downstream processes such as harvesting and refining (Fig. 1) and reduce their cost. For instance, when considering the harvesting steps, the setting and optimization of operating parameters are closely related to the knowledge of particle size distribution [22–24].

Downstream extraction processes (Fig. 1) are typically preceded by a cell disruption treatment (mechanical or non-mechanical) [25] aimed at breaking microalgal cells and facilitating the release of intra-cellular compounds [26–28]. Since the disruption reaction occurs at the cells' surface, mechanical and non-mechanical disruption techniques can be influenced by cell size [29,30]. Even the extraction of intracellular compounds is based on mass transfer phenomena occurring at the cell surface – liquid interphase and is thus strongly affected by the cell size. Therefore, starting from the knowledge of cell size distribution, one can finely tune the amount of energy and reactants used for cell disruption, thus reducing the operating costs.

When developing mathematical tools, the quantitative description of cell-to-cell heterogeneity can provide significant advantages for the design and control of microalgae cultivation and processing systems in the entire biorefinery process. Small cells attain higher photosynthetic and carbon fixation rates as compared to larger ones and are characterized by a faster uptake of nutrients [19]. Since nutrient absorption and light gathering occur at the cell surface, smaller cells are favoured compared to bigger ones due to their larger specific surface area. Single-cell biochemical analyses of microalgae have shown a high cell-to-cell variability in terms of proteins, lipids and starch content [16]. In some cases, the appearance of different subpopulations with different behaviour has been reported. Different works indicated that during N-starvation, the cell-to-cell heterogeneity for the accumulation of lipids increases in microalgae, thus significantly affecting the whole production rate of the population [17,31]. Population size structure may change even as a result of temperature or exposure to various pollutants, UV radiations, and other environmental conditions [32,33].

The mechanisms at the base of this high cell-to-cell heterogeneity are still largely unknown. Currently, no process control strategies are available to reduce the negative impact of cell-to-cell heterogeneity on microalgae process performances. The development of reliable and predictive mathematical models can shed light on these phenomena and possibly lead to effective control strategies in industrial bioprocesses. To this scope, the most powerful tool is represented by population balance equations (PBEs). The latter ones consist of a set of partial differential equations resulting from a dynamic balance of a population of individuals entities (cells) distinguished on the basis of one or more features, i.e. the so-called internal coordinates, which can be the cellular size, mass, age, morphology, etc. [34]. If the size is the internal variable, by using PBEs it will be possible to simulate the transient dynamics of a size-structured population of cells along with all the possible aspects discussed above.

An additional character of PBE-based models is that biomass growth and cell division are taken into account separately [19]. Such a feature may come in handy to properly simulate the cultivation of microalgae since, according to different studies [35–37], biomass growth and cell division can be uncoupled. This happens when microalgae face variable energy and nutrient availability (e.g. light/dark cycles) [35,37]. It should be noted that such behaviour cannot be described and predicted through classical unsegregated models, which do not distinguish between cell duplication and biomass production, thus leading to potentially unsuitable simulations. On the contrary, by allowing such a distinction, PBE-based models proposed in the literature [19,23] have been able to effectively simulate the effect of light-dark cycles on microalgae growth and division.

In light of the above, a systematic literature review is performed in this work on the use of PBEs in the microalgae-based processes. In particular, after a brief desciption of the general aspects of population balance tools, the work is articulated in three sections regarding the usage of population balance equations to quantitatively describe the three main steps of the microalgae technology, i.e. cultivation, harvesting and extraction. In addition to analysing the literature models based on the use of PBEs, the potential and perspectives for the application of this modeling approach for the analysis and

Table 1
Typical size ranges of some microalgal strains reported in the literature.

Strain	Parameter	Mean value	Min. value	Max. value	fold variation	Reference
Nannocholorpsis oculata	Volume (μm^3)	73.58	14.13	229.73	16.26	[19]
Tetradesmus obliquus	Volume (μm^3)	36	12	129	10.75	[17]
Tetradesmus obliquus	Volume (μm^3)	70	15	239	15.93	[17]
Tetradesmus obliquus	TAG content (pg/cell)	0.32	0.06	1.2	20	[17]
Tetradesmus obliquus	TAG content (pg/cell)	14	0.25	99	396	[17]
Chlorella sp.	Volume (μm^3)	57.88	44.58	82.41	1.85	[21]
Chlorella sp.	Volume (μm^3)	102.11	65.42	164.55	2.52	[21]
Chlamydomonas reinhardtii	Doubling time (h)	10	7	17	2.43	[18]

*TAG: Triacylglycerols.

optimization of the different microalgae processing steps are discussed.

2. The population balance equation (PBE)

The main goal of the PBE is to describe the evolution of a population of entities as a result of the action of external or internal factors [38]. External factors include temporal and spatial variations in the environmental variables (e.g., fluctuations in substrate concentration and external temperature in cell cultivation processes) that can influence the state of entities, while internal factors can be related to phenomena taking place within each entity (e.g., stochastic fluctuations in metabolites concentrations, asymmetric cell division). To describe the effect of these factors, PBEs rely on the number density function defined in a phase space including external and internal coordinates. PBEs literature refers to space coordinates$r = (x, y, z)$ as external coordinates, whereas the internal coordinates, hereafter denoted as $\zeta = (\xi_1, ...,\xi_n)$, coincide with one or more properties of the entities constituting the population, such as, for example, mass, size, age, energy, chemical composition and temperature [39].

By indicating with $\psi(r, \zeta, t)dr\, d\zeta = \psi\, |dS|$the total number of entities having coordinates in the phase space volume of size$|dS| = dr\, d\zeta = dx\, dy\, dz{\cdot}d\xi_1 d\xi_2 ... d\xi_n$, i.e., the space between (r, ζ) and $(r + dr, \zeta + d\zeta)$ at the time t, it can be stated that $\psi(r, \zeta, t)$ represents the so-called number density distribution in the space $\boldsymbol{S}$ [38]. Accordingly, the total number of entities in $\boldsymbol{S}$ is $\int S\psi\, |dS|$. Hence, by imposing the conservation law for the total number of entities, the following general formulation for the PBE can be derived [38,40–42]:

$$\frac{\partial \psi(r, \zeta, t)}{\partial t} + \nabla_r\, (\psi(r, \zeta, t)\, v_r(r, \zeta, t)) + \nabla_\zeta\, (\psi(r, \zeta, t)\, v_\zeta(r, \zeta, t)) = B(r, \zeta, t) - D(r, \zeta, t) \quad (1)$$

where $v_r = \left(\frac{dx}{dt}, \frac{dy}{dt}, \frac{dz}{dt}\right)$ and $v_\zeta = \left(\frac{d\xi_1}{dt}, ..., \frac{d\xi_n}{dt}\right)$ denote the velocity at which the entities move within the physical space and the rate at which internal coordinates change, respectively, while $B(r, \zeta, t)$and $D(r, \zeta, t)$ are the birth and the death rate of entities, respectively. In few cases, to take into account possible random fluctuations of the actual velocities, some authors [43–47] introduced also diffusive terms in the PBE thus obtaining the following general form:

$$\frac{\partial \psi}{\partial t} + \nabla_r\, (\psi v_r) + \nabla_\zeta\, (\psi v_\zeta) - \nabla_r\, (D_r\, \nabla_r \psi) - \nabla_\zeta\, (D_\zeta\, \nabla_\zeta \psi) = B - D \quad (2)$$

The diffusive terms come in handy, for example, in the case of plug flow reactors with dispersion [43] or for growth rates with stochastic components [48]. However, it should be noted that the correctness related to the introduction of diffusive terms in PBE is still a subject of a scientific dispute between different authors [44]. Accordingly, the classical general formulation of the PBE should be considered as the one reported in Eq. (1).

Finally, it should be noted that the deterministic formulations of velocities and source terms, i.e., birth and death, can be very different depending on the specific population being described (e.g., cells, particles, droplets), internal coordinates adopted (e.g., size, mass, age, temperature), as well as the specific phenomena being described (e.g., nucleation, growth, mitosis, breakage, aggregation, coalescence, birth, chemical reaction). A massive literature exists regarding the applications of PBEs to the most disparate systems, and its review is out of the scope of this work. On the contrary, our goal is to review the applications of PBE-modelling to microalgae-based processes and identify the possible applicative outcomes that can be derived from the use of PBE modelling in this emerging field.

3. Single-cell analysis

Every model needs to be validated against experimental data, hence in order to choose the internal coordinates to be used, it is fundamental to consider the experimental data that can be more easily and reliably obtained. Several different cell variables could be used as internal coordinates. The population balances for living cells have been typically written by using the cell volume as internal coordinate [34,40,46,48–54].

Frequently, the measurement of microalgae mass or cell number is carried out by optical density measurements. This technique mainly consists in generating a calibration curve between optical density measurement and cell dry weight or cell number, to be then adopted across the cultivation, providing an affordable and rapid tool for their measurement. However, these techniques show their limitations when it comes to evolving environmental conditions, which could affect pigments content, bringing a relevant error if the measurement wavelength is not properly chosen, and if the calibration curve is derived only ones for the whole set of experiments. If the calibration curve is not executed considering changes in pigments concentration and/or changes in the cell size within the cultivation, the measurement could not be representative of the real cell mass/number measurements introducing large errors [55,56]. In the case of PBMs applied to microalgae, different experimental techniques have been applied, based on the need of having accurate representation of the variable involved in the models, and specifically, of the cell mass/volume distribution. Typically, the analytical measurements for PBMs are carried out by using experimental techniques that overcome the limitations brought by spectrophotometric techniques. Hence, the use of specific techniques to measure cell mass/size distribution should enable to obtain accurate measurements of these variables excluding errors related to changes either in pigments content or size of the cells [55,56].

Cell volume can be measured directly or indirectly by using different techniques. For microalgae, these include the application of a cell counter, which measures the volume directly, or image-based cell-meters, which can be used to measure the area, diameter, volume or other morphological parameters, and flow-cytometers, which can be used to measure indirectly cell size/volume [54,57–59]. Flow-cytometry is a high-throughput method which can easily allow collecting up to 10,000 events/s, while the reliability of the results should be carefully assessed since the calibration of the instrument is more difficult compared to coulter counter and image-analysis. However, flow cytometers coupled to high-throughput image-analysis are commercially available (Attune CyPix, Thermo Scientific).

Mass is often used as an internal coordinate to describe the state cells in PBE models. In this case, experimental data for the mass distribution within the cell population are derived from volume distribution measurements by assuming a constantmass per unit of cell's volume, consequently assuming no variations of its own density. However, it should be taken into account that in many situations, density is not constant for microalgal cells, especially when microalgae are cultivated under temporally varying nutrient concentrations. In this case, microalgae can accumulate different amounts of starch (d = 1.5 g/mL) or lipids (d ~ 0.9 g/mL), which determines variations between the densities of cells. Density can also change in response to osmotic stress. Therefore, the assumption of constant density is only valid under some specific conditions.

Recent studies have shown the feasibility of measuring single-cell mass by measuring the cell's buoyant mass in H_2O and D_2O through a suspended microchannel resonator, which was applied to cells with weights between 10 fg up to 130 pg [60].

Other coordinates than size/volume and mass could also be used in the models, for example, cell's age, temperature, and chemical composition. However, their experimental quantification is more difficult. A few studies reported microalgal single-cell quantification

Table 2
Formulations of single-cell growth rates adopted in the literature for microalgae.

Expression of v_m adopted in the literature	Ref.
$\left[\mu_{\max}\frac{I_{av}^{n}}{K_I^{n}+I_{av}^{n}}\prod\frac{C_j}{K_j+C_j}\left(1-\frac{C_{O2}}{C_{O2}^{\max}}\right)-\mu_c\right]m$	[43]
$\mu_{\max}\frac{I_{av}^{n}}{K_I^{n}+I_{av}^{n}}\prod\frac{C_j}{K_j+C_j}\left(1-\frac{C_{O2}}{C_{O2}^{\max}}\right)m$	[66]
$\left[\mu_{\max}\prod\frac{C_j}{K_j+C_j}\frac{1}{H}\int_0^H\frac{I_{dir}(h)}{K_I+I_{dir}(h)}dh-\mu_c\right]m$	[58]
$\left[\mu_{\max}\frac{I_{av}}{K_I+I_{av}+\frac{I_{av}^2}{K_I''}}\prod\frac{C_j}{K_j+C_j}-\mu_c\right]m^{\frac{2}{3}}$	[19]
$\mu_{\max}\frac{I_{av}}{K_I+I_{av}}\frac{v}{K_v+v}-\mu_c v$	[59]
$\mu_{\max}\left[(1-x_A)\frac{(C_{NO_3^-}^{Int})^{n_L}}{(K_{C_{NO_3^-}^{Int},LG})^{n_L}+(C_{NO_3^-}^{Int})^{n_L}+\left(\frac{(C_{NO_3^-}^{Int})^2}{K_{C_{NO_3^-}^{Int},L:I}}\right)^{n_L}}+x_A\frac{(C_{NO_3^-}^{Int})^{n_H}}{(K_{C_{NO_3^-}^{Int},H})^{n_H}+(C_{NO_3^-}^{Int})^{n_H}+\left(\frac{(C_{NO_3^-}^{Int})^2}{K_{C_{NO_3^-}^{Int},H:I}}\right)^{n_H}}\right]\frac{I_{av}^{n_I}}{K_I^{n_I}+I_{av}^{n_I}+\left(\frac{I_{av}^2}{K_{I_{av}:I}}\right)^{n_I}}\left(\frac{3}{4\pi}\right)^{\frac{2}{3}}v^{2/3}$	[65]
$Constant=1$	[64]

of intracellular properties. Measurements have been reported for lipids, starch, proteins and DNA [16,17,61].

4. Application of PBEs for the optimization of the cultivation section

In this section, the development and application of PBE models to describe the growth of microalgae in the cultivation section are discussed. The literature survey initially analyses the application of univariate PBE models where either the size or the mass is used to describe the cell state, which is the approach most widely adopted by previous studies. Accordingly, Section 4.1 describes the size/mass structured PBE and the mathematical models used to simulate the continuous growth, birth and death terms appearing in this equation. The application of the structured size/mass PBE to describe microalgae growth with binary and multiple-fission is then reviewed in Sections 4.2 and 4.3, respectively. Finally, Section 4.4 discusses the application of PBE models, including the use of different internal variables, in addition to or alternative to the size/mass descriptions of the cell state.

4.1. Size/mass structured PBE mathematical modelling

Most works relying on PBEs take advantage of only one internal coordinate, which can somehow be traced back to the size (volume) or mass of the cells [38,44]. If this is the case, the PBE can be then derived to substitute the vector of internal coordinates ζ with m or v in Eqs. (7)–(8), respectively. Particularly, as living cells were concerned, the cell volume v (or, equivalently, the diameter or the surface area) was typically used as internal coordinate in PBE models [34,40,46,48–54]. This choice was mainly motivated by the wider availability of cell size/volume distribution data derived by the application of cell counter, image based cell-meters, and cyto-fluorimetry [54,57–59]. The use of the mass as an internal coordinate for PBE modelling of living cells is, in contrast, less common, even though some relevant papers demonstrated that it permits obtaining simpler expressions for the growth and source/sink terms [38,53,57,62,63]. On the other hand, when the density of cells is assumed to be constant during the simulated process, mass and volumes are linearly dependent; thus, the volume and mass-structured PBEs become equivalent.

Motivated by this analysis, with only a few exceptions [59,64,65], PBEs so far proposed in the microalgae literature were written using the cell mass m as the internal coordinate [19,43,58,59,64,66,67].

Broadly, CSTR photobioreactors were considered in these works, and thus the convective term in space at the LHS of Eq. (2) disappears. Under these conditions, by integrating both sides of Eq. (2) over the reactor volume, the following PBE can be derived:

$$\frac{\partial\psi(\xi,t)}{\partial t}+\frac{\partial}{\partial\xi}\left(\psi(\xi,t)v_\xi(\xi,t)\right)=B(\xi,t)-D(\xi,t)-Dil(t)\psi(\xi,t) \tag{3}$$

where ξ represents m or v depending on whether the volume or the mass is used as an internal coordinate, and $Dil(t)$ denotes the reactor dilution factor. In what follows, the approaches adopted in the literature to describe continuous growth (v_m or v_v), as well as birth (B) and the death (D) terms are reviewed.

4.1.1. The continuous growth term

The second term on the LHS of Eq. (3) takes into account the fact that the mass, m, and the volume, v, of a single cell increase continuously with rates $v_m=\frac{dm}{dt}$ or $v_v=\frac{dv}{dt}$, respectively, contributing to changing over time the corresponding density distribution functions [68]. These rates depend on different variables, including the limiting nutrient concentration in the growth medium (C_j), the average light intensity within the culture (I_{av}), the dissolved oxygen concentration (C_{O2}), and the intracellular nutrient concentrations (C_j^{Int}) [43,58,66]. As shown in Table 2, different expressions have been used to evaluate the volume growth rate of single cells.

As can be observed from Table 2, except for a few differences, the adopted expressions were quite similar. In these Equations, $\mu_{\max}$ represents the maximum specific growth rate, while μ_c is the continuous rate of mass loss. The latter one can be attributed to specific physiological phenomena such as respiration, maintenance and catabolites excretion, and it was typically assumed to be constant. A Monod-type expression was usually adopted to quantify the dependence of $v_m$on the nutrient concentrations in the growth medium, except for Usai et al. [65]. In the latter study, v_m adoptes a double affinity law to describe the ability of microalgae to growth at high and low levels of intracellular nitrates concetrations. The dependence on the intracellular nutrient concentration was introduced to simulate the ability of microalgae to grow by exploiting

accumulated reserve materials even when a limiting nutrient is depleted in the extracellular environment. This dependence is usually described by the Droop model, typically used to simulate microalgae growth under depletion of N or P [9,69]. Hill, Haldane, or modified Andrews-type dependence were adopted for the light-dependent kinetics [70]. Using these functional forms allows for the accounting of potential photo-inhibition phenomena occurring at too-high light intensities. Finally, the inhibition effect of oxygen was typically accounted for by a saturating function, when the photobioreactor type can determine oxygen accumulation in the liquid phase.

An aspect to observe in the Equations of Table 2 is that cell mass v_m or volume v_v growth rates are typically assumed to increase linearly with the mass or size of the cell [43,58,66]. However, the dependence of the growth rate on the 2/3 power of the mass (or size) was often reported to more effectively describe the effect of cell size/mass on growth kinetics [71]. Indeed, the nutrient uptake rate of microalgae increases linearly with the number of sites for nutrient uptake available at the cell surface [72]. Since the surface density of these sites can be considered constant during cell growth, the nutrient uptake rate of a microalgal cell increases linearly with the area of the cell surface which, in turn, is proportional to a 2/3 power of the cell volume and thus of cell mass [73]. Light supply, needed to trigger photosynthesis, also depends on the geometric cross-section of the cell, and therefore it is proportional to the 2/3 power of the volume as well [74]. Accordingly, in the late formulation by [19], a 2/3 allometric scaling law was adopted for the cell mass.

4.1.2. Death and birth terms

The term D at the right-hand side of Eq. (3) takes into account that a cell of mass m can disappear as a result of its division, due to mitosis, into a certain number of daughter cells having smaller masses (or sizes). For size or mass-structured PBEs, this term can be expressed as the product between$\psi(m)$and the so-called division intensity function (Γ)representing the propensity of cells to divide as they approach a certain critical mass(m_c).

$$D(m) = \Gamma(m)\psi(m) \tag{4}$$

In one of the reported cases of size-structured PBEs [75], the same relationship was adopted, while all the functions were assumed to depend on a typical characteristic length of microalgae cell, and $\Gamma$was assumed to remain constant.

When mass was considered as the only internal coordinate [43,58], the function Γ was expressed as the product of a division rate v_d, typically considered equal to the single cell growth rate, and the probability that the cell divides depending on its mass:

$$\Gamma(m) = v_d(m, C_j, I)\frac{f(m)}{1 - \int_0^m f(m')dm'} \tag{5}$$

The function $f(m)$returns the probability density that a cell divides when its mass, m, approaches the critical one (m_c)and is, in these cases, expressed as a Gaussian function:

$$f(m) = \frac{1}{\sqrt{2\pi\sigma_c^2}}\left[-\frac{(m - m_c)^2}{2\sigma_c^2}\right] \tag{6}$$

The symbols σ_c refers to the standard deviation of dividing mother cells. It should be noted that Eqs. (4)–(6) can be equivalently expressed by using the cell volume (v) instead of the cell mass(m). The following sections will provide more details related to some of these alternative formulations.

In Eq. (3), the symbol B represents the birth rate and takes into account the contribution to the class of cells with mass (m) (or volume v) by newborn cells resulting from the division of cells having larger mass $m' > m$ (or volume $v' > v$). The probability that a cell having mass m is formed depends on the rate $D(m') = \Gamma(m', Cj)\psi(m')$ at which the larger cells, i.e., with $m' > m$ (or $v' > v$) undergo cytokinesis as well as on the fraction $p(m, m')$ (or $p(v, v')$) of cell having mass m produced by the division of the cell with mass m'. Since each cell with mass $m' > m$ (or $v' > v$) might theoretically divide to give rise at least one cell of mass m, the overall contribution of newborn cells to the class of cells with mass m or volume v is obtained by integrating this contribution over the mass domain involving all the cells having mass $m' > m$ or volume $v' > v$.

Therefore, the birth term B in the population balance can be written as follows:

$$B(m) = \int_m^\infty \Gamma(m', C_j)\, p(m, m')\, \psi(m')\, dm' \tag{7}$$

The so-called partition function $p(m, m')$ thus expresses the probability that a mother cell of mass m' will give birth to a daughter cell of mass m when it divides. As far as microalgae are concerned, the expressions reported in Table 3 have been adopted in the literature for the partition terms.

It should be noted that the expressions in Table 3 are representative of a situation, called unequal partitioning, where the daughter cells produced at each division cycle can have different size.

If the case of binary fission with equal partitioning is considered, i.e., two daughter cells having the same mass are produced by each mitotic event, the Eq. (7) can be simplified as follows [34]:

$$B(m) = 4\,\Gamma(2m)\,\psi(2m) \tag{8}$$

This assumption permits simplifying the numerical handling of the resulting PBE model. With all of these considerations, the typical PBE can be solved along with the corresponding initial and boundary conditions. It should be noted that, while the initial condition is given by the initial distribution of cells, the typical boundary condition is $\psi(0, t) = 0\ \forall\ t$, expressing the condition that no cell with null mass or volume should be taken into account.

Table 3
Expression adopted in the literature to describe the partition function of microalgae.

Expression of p (m,m')	Symbol significance / notes	Ref
$\frac{1}{\beta(q,q)}\frac{1}{m'}\left(\frac{m}{m'}\right)^{q-1}\left(1-\frac{m}{m'}\right)^{q-1}$	Binary fission m: mass of the cell $(g)m'$: mass of the mother cell $(g)q$: parameter of the beta function $(-)\beta$: Euler beta function	[43]
$30\frac{m^2(m'-m)^2}{m'^5}$	Binary fission m: mass of the cell $(g)m'$: mass of the mother cell (g)	[58]
$\frac{1}{\beta(\alpha_i,\delta_i)}\frac{1}{m'}\left(\frac{m}{m'}\right)^{\alpha_i}\left(1-\frac{m}{m'}\right)^{\delta_i}$	Multiple fission in terms of mass. m: mass of the cell $(g)m'$: mass of the mother cell $(g)\alpha_i$, δ_i: parameters of the beta function for division into i daughter cells $(-)\beta$: Euler beta function	[19]
$\frac{1}{\beta(\alpha_i,\delta_i)}\frac{1}{v'}\left(\frac{v}{v'}\right)^{\alpha_i}\left(1-\frac{v}{v'}\right)^{\delta_i}$	Multiple fission in terms of mass. v: volume of the cell $(g)v'$: volume of the mother cell $(g)\alpha_i$, δ_i: parameters of the beta function for division into i daughter cells $(-)\beta$: Euler beta function	[65]

4.2. Application of the size/mass structured PBE model with binary cell division

As far as the application of PBEs to microalgae is concerned, the first work presented in the literature was the one by Concas et al. [43]. In this work, a classical homogeneous, isothermal, axial dispersion model was adopted to simulate the spatiotemporal evolution of main nutrient species (C, N, P) and photosynthetic O_2 in the liquid phase in a BIOCOIL photobioreactor. A PBE model was adopted to simulate algae growth. In particular, since microalgal cells move along the tube, a "mass structured" population balance, including the effect of cell dispersion along the reactor axis, was proposed:

$$\frac{\partial \psi}{\partial t} + \frac{\partial (\psi v_m)}{\partial m} + v_z \frac{\partial \psi}{\partial z} - E_{D,z} \frac{\partial^2 \psi}{\partial z^2} = B - D \tag{9}$$

where z denotes the axial coordinate, while $v_z$and $E_{D,z}$represent the velocity and the dispersion coefficient along the z-direction, respectively. Accordingly, a 2D-PBE was obtained with the z-direction as external (spatial) coordinate and the cell mass(m)as the only internal coordinate. Birth and death terms were described by Eqs. (4) and (7) with division intensity and partition functions reported in Eq. (5), and Tables 1–2. The 2D-PDE system resulting from coupling the PBE to the mass balances for nutrients and oxygen was then solved by the application of finite element techniques [43]. The solution returned the number density function Ψ from which the biomass concentration X could be computed as follows:

$$X(z, t) = \int_0^\infty \psi(m, z, t) m dm \tag{10}$$

The reliability of the mathematical model was assessed by comparison with experimental literature data, expressed in terms of biomass concentration, concerning the growth of the cyanobacteria *Spirulina Platensis* in BIOCOIL [76]. However, the comparison could not be performed in terms of mass distribution since no experimental data were available for such distribution. On the other hand, by analysing the evolution of the mass distribution at the reactor outlet predicted by the model (Fig. 2a), the mechanisms responsible for transient oscillations (Fig. 4b) in the outlet biomass concentration reported by previous experimental studies [76] could be explained. In accordance with the illustrated analysis, these oscillations can originate from the initial overlapping of mitosis and growth within the cell population, and they are progressively damped as cells get synchronized (i.e., mitosis and growth take place at the same time for all the cells).

Bertucco et al. [58] applied a PBE model to simulate and control *Scenedesmus obliquus* growth in a flat panel photobioreactor operated in both batch and continuous modes. Again, only the mass was employed as an internal coordinate, and the implemented PBE was thus substantially equal to Eq. (3). The single cell mass growth rate and the partition function adopted to describe birth and death terms are reported in Tables 2 and 2, respectively [58]. The PBE was solved through the Finite-size domain Complete set of trial functions Method of Moments (FCMOM) [77].

In Bertucco et al. [58], the PBE model was validated for the first time not only by comparing the predicted and experimental biomass concentrations but also in terms of mass distribution. To this aim, growth experiments were performed during which cell size and mass distributions were recorded by the application of a cell counter. The critical mass, i.e., the mass at which cells divide, was varied at selected residence times to enforce the fitting of the model to experimental biomass and cell concentrations. This aspect might be questionable since the critical mass should always be the same for the same microalgal strain. However, some authors confirm that a slight change in the critical mass can be observed depending on the cultivation conditions. In addition, it should be noted that, by adopting this fitting strategy, the model could satisfactorily reproduce not only the evolution of average cell and wet biomass concentrations, but also the mass distribution experimental data. The latter data were not used to perform the fitting, which contributes to corroborate the reliability of the analysis presented by Bertucco et al. [58].

4.3. Application of the size/mass structured PBE model with multiple fission

The models so far discussed are based on the assumption that microalgae strains divide by binary fission, which is valid only for some species and under particular environmental conditions. Several microalgal species, such as *Scenedesmus* and *Desmodesmus*, show alternative cell cycles, whereby they divide into 2^n daughter cells, with n ranging between 1 and 15 (multiple fission).[37,78,79]. To the best of our knowledge, only three mathematical models of microalgae growth taking into account multiple cell division have been proposed in the literature [19,80,81] with two of them considering also the life-cycle of microalgae cells [81,82].

While well-posed from the mathematical point of view, the model by Rading et al. [80] neglects relevant biological phenomena, such as the effects of light intensity and nutrient concentrations on

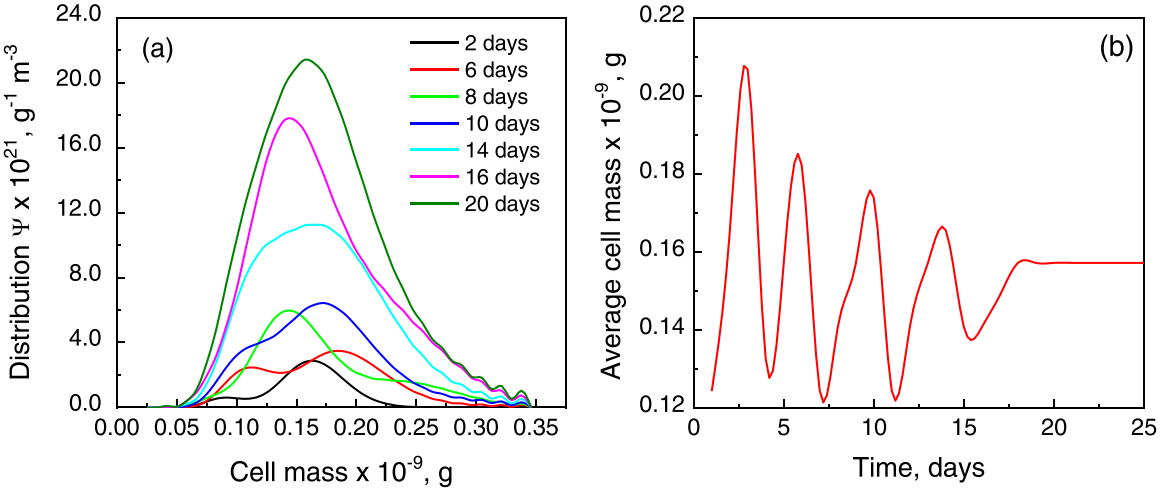

Fig. 2. Cell mass distribution at outlet (z = L) of the biocoil photobioreactor (a), and average cell mass oscillations over the cultivation time (b). Adapted from Concas et al. [43].

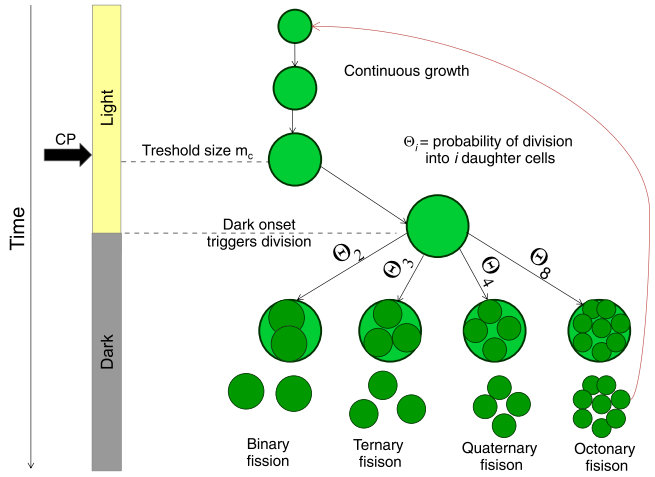

Fig. 3. Scheme of main phenomena involved in microalgae cell division by multiple fission.
Adapted from Concas et al. [19].

the growth of single cells and the occurrence of cell division in the dark.

On the contrary, the model by Concas et al. [19] considered the effect of different operating parameters and culture conditions, such as, for example, light intensity and nutrient availability, to simulate the size-structured growth of the strain *Pseudochloris wilhelmii* dividing by multiple fission. The model is based on some specific features of the microalgae cell cycle schematically shown in Fig. 3. When exposed to light, cells exploit photosynthesis to increase their size (G1 phase). At a certain instant, hereafter called commitment point (CP), cells attain the minimum size that allows triggering a sequence of events leading to cell division. Specifically, cells can enter the S, G2 and M phases and finally divide by cytokinesis. However, when the CP is reached during the light period, the division process is postponed in order to prevent possible DNA damage phenomena induced by the photon flux [37]. If this is the case, then the cell continues to grow rather than divide, and consecutive CPs can be attained. Each CP is followed by DNA replication-division, but only at the onset of dark (or very low light intensity) the cells can perform cytokinesis and release the new-born daughter cells. The number of new-born daughter cells is then roughly equal to 2^n, n being equal to the number of CPs previously attained.

However, the mechanisms governing the progression through the cell cycle and determining the number of attained CPs are still not completely clear, and a biologically sound mathematical model which allows predicting how many cells are formed at each mitotic event is not available. On the other hand, the frequency with which each mitotic event gives rise to a specific number of daughter cells can be determined from experimental data of cell division. Such an approach was exploited by Concas et al. [19] to infer the probability (Θ_i), that the division generates a given number (i) of daughter cells for a concerned strain. The general formulation of the PBE described by Eq. (3), with the growth rate depending on light intensity, nutrient availability and cell mass (Table 2), was adopted by [19]. However, the death term D, describing the disappearance of a cell of mass m as a result of division, was modified as follows (Eq. (11)) to ensure that division could occur only at a sufficiently low light intensity to prevent DNA photodamage:

$$D(m) = \mu_{\max} \prod_{j=1}^{2} \frac{C_j}{K_j + C_j} m^{\frac{2}{3}} \frac{f(m)}{1 - \int_0^m f(m')dm'} [1 - H(I_{av})]\Psi(m) \tag{11}$$

where $H(I_{av})$ is the Heaviside function of light intensity. To describe the possibility of multiple-fission, the birth term was then written as follows:

$$B(m) = \int_m^\infty \Gamma(m', C_j) \frac{1}{m'} \vartheta(m, m') \Psi(m') dm' \tag{12}$$

where $\vartheta(m, m')$ denotes the self-similar daughter distribution and obeys the extended Hill-Ng power law [19]. This distribution contemplates the possibility that a variable number (i) of daughters cells may be generated and can be written as follows:

$$\vartheta(m, m') = \sum_{i=1}^{n_d} m'\, i\ \Theta_i\ p_i(m, m') \tag{13}$$

where $p_i(m, m')$ is the partition function and is clearly defined in Table 3. By substituting expressions Eq. (12) and Eq. (13) in Eq. (3), the following PBE can be derived:

$$\frac{\partial \psi}{\partial t} + \frac{\partial (v_m \psi)}{\partial t} = -\Gamma(m, C_j)\psi + \sum_{i=1}^{n_d} i\, \Theta_i \int_m^\infty \Gamma(m', I, C_j)\, p_i(m, m')\, \Psi(m')\, dm' \tag{14}$$

To validate the model, the simulation results were compared with the experimental data derived by monitoring the growth of the strain *Pseudochloris wihlelmii*, typically dividing by multiple fission, in batch photobioreactors where the growth rate limiting nutrients were nitrates and phosphates. Only the maximum growth rate was estimated by fitting model predictions to the experimental data obtained under a base condition, while the remaining model parameters were taken from the literature [19]. Since no experimental data were available for the size distribution, model validation could only be performed by verifying the ability to predict average biomass concentration data (Fig. 4a). Nonetheless, the model could effectively describe the decoupling of biomass growth and cell division steps between the day and the night, predicting oscillations of the average diameter (Figs. 4b, 4c), which are qualitatively in agreement with experimental findings [19].

Finally, in order to show the capability of PBE modelling to optimize the microalgal technology Concas et al. [23] evaluated the effect of the cell division mode on the dosage of flocculant needed to achieve and effective harvesting. The results of such an analysis are here summarized in Fig. 4d. This figure highlights how the cell division mode, and thus the size distribution affects the amount of flocculants needed to harvest microalgae and thus the economic sustainability of the process. Ultimately, while needing to be further corroborated by experimental evidence, the model by Concas et al. [19] permits to suitably account for the effects of multiple fission on industrially relevant aspects of microalgae cultivation.

Usai et al. [65] presented a PBE based on the same fission modelling framework proposed by Concas et al. [19,23] but using the cell volume as the principal internal coordinate. However, their model considered two distinct compartments, i.e., an intracellular and an extracellular compartment, which exchange nutrients along with light. The model potentially allows the description of intracellular products not secreted in the extracellular environment as well as the time evolution of nutrients in the extracellular compartment that are available for cell uptake and intracellular processes. The PBEs followed the same form of Eq. (3) except for the addition of a lysis term, which depends on nutrient availability, to account for the cell number decrease experimentally observed. One of the main specific aspects of the model consisted in the coupling of cell growth with the extracellular and intracellular nutrient content by means of Eqs. (15) and (16), where total volume V^T_{Cells} was evaluated through the PBE:

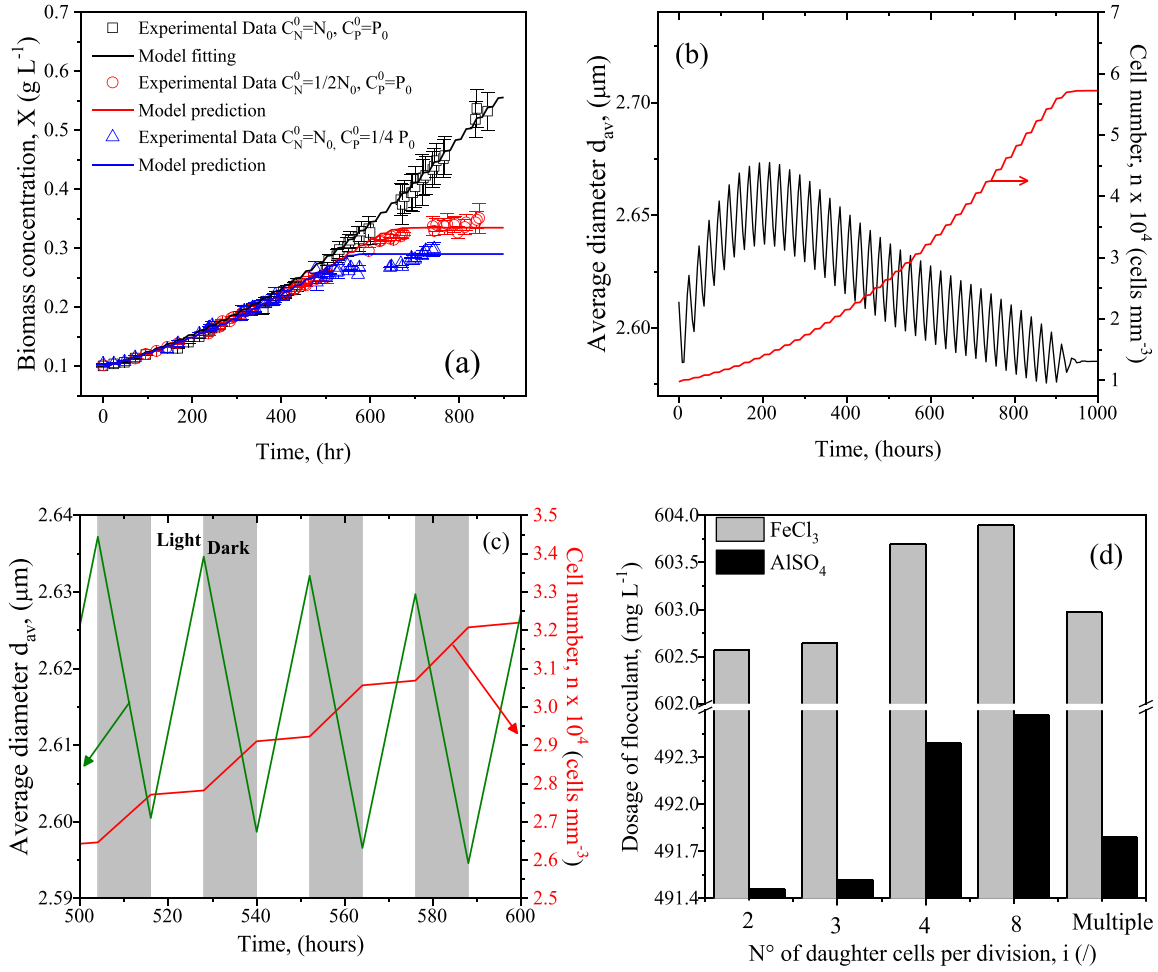

Fig. 4. Results obtained with the model by Concas et al. [19,23] by simulating multiple fission of microalgae: comparison between model results and experimental data in terms of first moment of the distribution (a); dynamic evolution of average cell size and cell number (b) and effect of light – dark photoperiod on the average cell size and cell number evolution (c); effect of the cell division mode on the dosage of flocculant needed to harvest microalgae
Adapted from Concas et al. [19,23].

$$\frac{dc_j^{Med}}{dt} = \frac{1}{V_R^T - V_{Cells}^T}\left(c_j^{Med}\frac{dV_{Cells}^T}{dt} - \dot{C}_j\right) \tag{15}$$

$$\frac{dc_j^{Cells}}{dt} = r_{G,j} + \frac{1}{V_{Cells}^T}\left(\dot{C}_j - c_j^{Cells}\frac{dV_{Cells}^T}{dt}\right) \tag{16}$$

Here, the material balances for the specific *j-th* species are carried out in the specific control volume for the cells (V_{Cells}^T), and for the cultivation medium ($V_R^T - V_{Cells}^T$). Also, the transport of the species between the two compartments is considered throughout the term $\dot{C}_j$, as well as the dilution term due to variation of the cell population volume, indicated here as a derivative of the total cell volume $\left(\frac{dV_{Cells}^T}{dt}\right)$.

Model predictions showed a good agreement with experimental data in terms of 0th order moment, of average cell volume (ratio between order 1st and 0th), and nutrient availability in the extracellular media.

The model prediction was also tested against the experimental density distribution of the cells (Fig. 5) recorded during the photoautotrophic cultivation of *Haematococcus pluvialis*. To the best of our knowledge, as far as microalgae are concerned, this was the more comprehensive comparison of PBEs model results, in terms of cell size distributions, with experimental data. Furthermore, the proposed model was able to predict the relevant lyses phenomena, occurring when cells undergo stress nutrient conditions. This aspect is a relevant advantage of the model since lysis can dominate useful products loss if not properly addressed.

Further improvements of this model could be obtained as intracellular nutrient data become available. These data could allow refining model calibration and validation for all the variables involved.

4.4. Beyond size/mass structured PBE models of microalgae growth: introduction of additional/alternative internal variables

All the studies analysed in the previous section included the application of the size/mass structured PBE model, where only the mass or the volume defines the cell state. However, this is a simplification of how internal coordinates can represent the physiological response of cells (e.g., biomass composition) that cannot be unequivocally quantified based on the knowledge of only the size/mass. Cells with the same mass or volume, but attaining different values of these internal coordinates, can thus exhibit different responses (e.g., growth rates) to identical perturbations in the environmental variables. Tracking the evolution of the cell mass or volume distribution may be then insufficient to predict how cell heterogeneity is structured in response to the temporal evolution of environmental variables. In this framework, experimental studies have demonstrated that significant variations in the cell response to external perturbations can be attained depending on the position

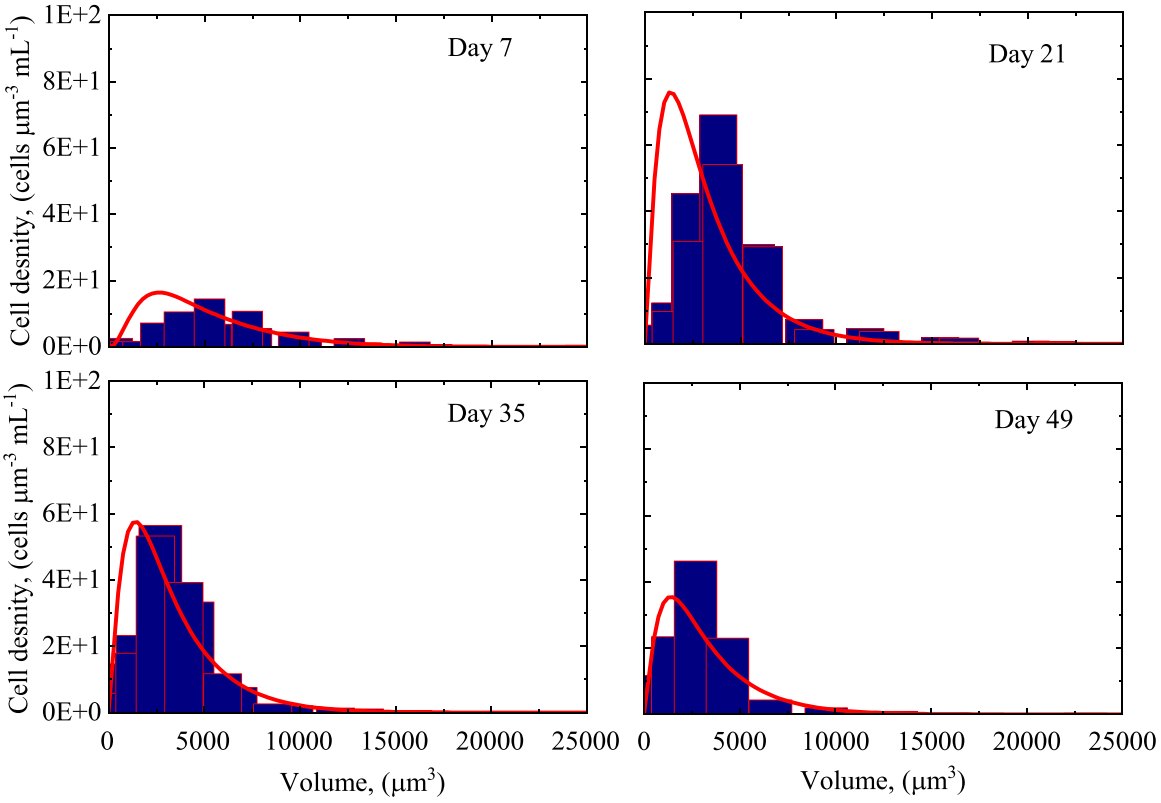

Fig. 5. Model predictions in terms of density distribution comparison between model and experimental data adapted from Usai et al. [65].

within the cell cycle and/or the biomass composition (e.g., internal quota of reserve materials).

4.4.1. The impact of cell cycle structure on microalgae population dynamics

Cell duplication and growth take place separately within the different stages of the cell cycle. While depending on the specific strain, the cell cycle of microalgae is generally characterized by four main phases that are common to all strains [83]. Growth of single-cell size occurs in the G1 phase due to the conversion of assimilated nutrients into structural intracellular molecules, among which mRNA and proteins that are required for DNA synthesis. When these reactions are completed, and the cells reach a critical mass/size (commitment point), the cells are committed to divide, and they can pass to the following S-phase where DNA is duplicated [51]. During this phase, nutrients uptake and cell size growth are interrupted since only internal transformations take place within the cell. At the end of this process, cells achieve the so-called G2 phase, wherein proteins and other cellular components needed for cell division are synthesized. Therefore, a certain increase in the cell size/mass occurs in this phase, which is typically lower than in G1 phase. Finally, the cells enter the M phase (mitosis), where each cell divides (cytokinesis) into two daughter cells. In this phase, no cell mass increase occurs, while cell number increases can be observed following division. Then, each new-born daughter cell reiterates the cycle described above [37,83,84].

According to this qualitative description, environmental factors (nutrient concentration and light intensity) control the progression through only specific cell cycle stages. This aspect explains why cell division can take place after nutrient starvation is introduced [85]: the cells that have already completed the growth phase and crossed the CP are allowed to divide.

This dynamics can hardly be described by the size/mass structured PBE formulation discussed in the previous section. In the application of this formulation, the velocity of cell division is typically assumed to be equal to the cell growth rate, which becomes equal to zero under nutrient starvation. This implies that cell duplication is allowed only in case nutrients are available, which is in contradiction with the experimental evidence. It should be also observed that, by employing only the size/mass as internal coordinate, the PBE formulation can be hardly corrected to describe illustrated mechanisms of progression through the cell cycle. While a critical mass/size threshold can be used to identify the achievement of the CP, the mass remains constant during the S and the M phases and cannot thus be used to track the progression through these stages of the cycle. The approach that has been followed to overcome this obstacle is to introduce, alternatively or in addition to the cell mass/size, an internal coordinate identifying the position within the cell cycle.

A PBE formulation, including the application of only this internal coordinate, was implemented by [86] to investigate the impact of the cell cycle on the dynamics of a microalgae population in a CSTR. It was assumed that, during the nutrient-dependent segment, progression through the cycle proceeds at a rate depending on the external concentration of a limiting nutrient through a Monod-like function, while the progression rate is constant during the nutrient-independent segment. Accordingly, the PBE was written as follows:

$$\frac{\partial \psi}{\partial t} + \frac{\partial (v_p \psi)}{\partial p} = -D(p)\,\psi - Dil\,\psi \tag{17}$$

where p denotes the position within the cell cycle, while v_p is the rate of progression through the cycle, which was expressed as follows:

$$v_p = \begin{Bmatrix} v_0 \frac{C_N}{K_N + C_N} \; if \; p \in [p_0, p_c] \\ v_c \; if \; p > p_c \end{Bmatrix} \tag{18}$$

where v_0, v_c and K_N denote the maximum progression rate during the nutrient dependent segment, the progression rate during the resource independent segment and the half-saturation constant, respectively. Cell division was described by the following boundary condition expressing the flux of new-born cells at $p = 0$:

$$\frac{dp}{dt}\psi(p, t) = 2\int_0^\infty D(p')\psi(p', t)dp' for p = 0 \tag{19}$$

while the function $D(p')$ was written as follows:

$$D(p) = \left[\frac{dp}{dt} \frac{f(p)}{1 - \int_0^p f(p')dp'} \right] \tag{20}$$

where $f(p)$ is the normal distribution described by Eq. (6) with the mass m replaced by p..

By considering model simulations, it was shown that autonomous periodic oscillations in the cell concentration can be generated in the CSTR by the interaction between the dynamics of nutrient consumption in the medium and the cell distribution along the cycle. The model was subsequently runned by including the periodic forcing of the inlet nutrient concentration. Under these conditions, the onset of quasi-periodic and chaotic oscillations was observed. However, the study did not include any systematic comparison, even qualitative, with the outcomes of experimental studies.

The model proposed by [86] was successively adopted by [87] to qualitatively explain the synchronization of microalgae cells in response to the alternation of nutrient replete and nutrient starvation conditions. In this study, it was experimentally demonstrated that starting from a population of non-synchronized microalgae cells, the transient application of nitrogen starvation, followed by the replenishment of nitrogen, allows attaining synchronized growth and replication. By the application of the model proposed by [86], the authors showed that the synchronization can be explained by arrested progression through the cell cycle attained under nitrogen starvation: cells starting from different positions within the nutrient-independent segment of the cycle eventually reach and accumulate at the beginning of the nutrient-dependent segment. Starting from the latter condition, synchronized progression through the cell cycle can then be activated by the replenishment of nitrogen.

While qualitatively reproducing microalgae population dynamics, the PBE formulation with the cell state described by the only position within the cycle can hardly be validated against experimental data or implemented for process control objectives. It is indeed difficult to monitor the position of cells within the cycle. To overcome this limitation, [66] proposed a PBE model with two internal variables: the cell mass and the position within the cell cycle. The main advantage of this approach is the possibility to effectively parametrize the progression through the cell cycle by the position coordinate, reproducing, at the same time, the mass distribution of cells, which can be used for model validation and/or control purposes.

The model was split into two main PDE equations (Eqs. (21)-(22)). The first one (Eq. 21) is valid when the cell mass is lower than the critical one ($m < m_c$) and the second (Eq. 22) works for the nutrient-independent phase, i.e., for $m \geq m_c$:

$$\frac{\partial \psi}{\partial t} + \frac{\partial (v_m \psi)}{\partial m} + \frac{\partial}{\partial p}\left(\frac{v_m}{m} \psi \, p_{ref}\right) = -D \, \psi - Dil \, \psi \, for \quad m \in [0, m_c] \tag{21}$$

$$\frac{\partial \psi}{\partial t} + \frac{\partial (v_m \psi)}{\partial m} + \frac{\partial \left(\mu_{max} \psi \, p_{ref}\right)}{\partial p} = -D \, \psi - Dil \, \psi \;\; for \;\; m > m_c \tag{22}$$

Here p_{ref} represented the minimum cell maturation degree which allows division, and *Dil* denotes the dilution rate, introduced to simulate fed-batch mode operation. The death rate D was evaluated as:

$$D = \left[\frac{dm}{dt} \frac{f(m)}{1 - \int_0^m f(m')dm'} + \frac{dp}{dt} \frac{f(p)}{1 - \int_0^p f(p')dp'} \right] \psi \tag{23}$$

where $f(p)$ is the normal distribution (Eq. 6). The birth term B does not appear in the PBEs (Eqs. (21)-(22)) since it was considered in the boundary conditions as follows:

$$\psi(m, p, t) = 0 \;\; for \;\; m = 0 \tag{24}$$

$$B = \frac{dp}{dt} \psi(m, p, t) = 2\int_0^\infty D(m, p', t) \, \psi(m, p', t) \, dp' \, for \; p = 0 \tag{25}$$

The numerical solution of the proposed model by finite difference techniques permitted evaluating the evolution of the cell distribution function during batch operation in the domain of the mass and the cell position within the cycle. Moreover, the total biomass concentration and nutrient consumption were evaluated under batch operating conditions. Finally, the fed-batch operation was simulated by considering different harvesting periods to identify the dilution ratio that maximizes biomass productivity. The model was very innovative in the microalgae sector, both in light of the considered phenomena and the theoretical framework developed despite the fact that the obtained results were not validated by comparison with experimental data.

4.4.2. The impact of internal nutrient quota on microalgae population dynamics

The response of cells to changes in the environmental variables can vary depending on the internal composition. For example, cells can undergo lysis or survive under nutrient starvation depending on whether they have previously accumulated sufficiently large fractions of reserve materials (e.g., lipids, carbohydrates). This mechanism is extensively exploited for the selection of microbe strains with an increased ability to accumulate reserve materials starting from mixed microbial populations [88]. To this aim, feast and famine processes are typically implemented, whereby nutrient replete conditions (feast phase) are alternated to nutrient starvation (famine phase). This way, microorganisms that accumulate larger fractions of reserve materials during the feast phase can be selected during the famine phase over the microorganisms with reduced accumulation capacity. This strategy is typically implemented with the objective of selecting a specific strain from a mixed culture, while a different response to temporal variations in the external nutrient concentrations can be observed even starting from a unique strain. [85] have recently applied the feast and famine strategy to prevent bacterial contamination during the heterotrophic cultivation of microalgae. For both bacteria and microalgae, only a fraction of the cells were found to undergo lysis during the famine phase, while the remaining cells could resist starvation for a significantly longer period, thus suggesting the existence of sub-populations with different resistances to starvation. Although a definitive explanation for this experimental result is currently elusive, reported experimental results suggest that the existence of two subpopulations with markedly different resistances to starvation might have been determined by a heterogeneous distribution of the reserve material accumulation during the initial feast phase [85].

The idea that temporal fluctuations in the nutrient availability or the application of nutrient starvation could activate a heterogeneous behaviour, typically referred to as "phenotypic heterogeneity", of isogenic cells has been, at the same time, consolidated by single-cell experimental studies [89].

Unfortunately, scarce attention has been paid to the development of PBE mathematical models describing the distribution of internal biomass fractions within the cell population. In this framework, a PBE model making use of the nitrogen quota q as an internal coordinate was implemented by [90] to examine the impact of a heterogeneous distribution of the microalgae cell composition. This modelling approach was guided by the idea that the growth kinetics of each cell within the population can be described more effectively by the Droop model than by a Monod-like model. The Droop model, which is the most widely adopted to describe the unsegregated growth of microalgae biomass [9], is based on the assumption that the internal quota determines the growth rate, and not the external concentration, of nitrogen. The internal nitrogen quota q varies within a prescribed interval $[q_{min}, q_{max}]$ and provides an indirect quantification for the fraction of accumulated reserve materials: the fraction of reserve materials progressively increases with decreasing q from q_{max} to q_{min} [91]. In the PBE model proposed by [90], microalgae population dynamics were described by the introduction of a biomass density function with internal coordinate the nitrogen quota q. Accordingly, the model does not provide any indication about the mass distribution and does not describe the impact of cell division, quantifying only the part of the biomass contained in the reactor volume that has prescribed nitrogen quota, q. The analytical solution of the proposed PBE model was compared with the solution of the unsegregated reactor model derived by the application of the Droop model with an average nitrogen quota. This way, the overestimation of the growth rate produced by the Droop model with the average quota was quantified. The study, however, did not include any comparison between model predictions and experimental results.

5. Application of PBE models to the design of downstream processes

5.1. Use of PBEs for the design of the harvesting section

Harvesting is one of the most expensive section of the entire microalgae-based process, especially in the cultivation plants making use of open ponds, where lower biomass concentrations (high water content) are attained [92]. Accordingly, the identification of proper techniques to harvest microalgae is crucial to increase process sustainability. One of the main aspects of the harvesting is related to the cell movement within the fluid containing themselves. The description of the cell movement in a liquid media can be challenging and its complexity increases dramatically when factors such as shape, motility, cell density, equipment design become relevant and need to be considered. A comprehensive reading on the topic to be considers is Dusenbery's book [93]. At the photobioreactor or pond outlet, the culture medium has a water content typically ranging between 99.5% and 99.9%. Different methods are typically employed for microalgae harvesting; a brief summary is reported in Table 4.

Harvesting efficiency is strictly related to the size of particles or particle aggregates (flocs) to be separated from the liquid phase. Indeed, when considering filtration systems, only flocs larger than the pores of membranes or cakes can be separated. On the other hand, in the case of gravity settling or centrifuges, recovery yields depend on the rate at which flocs move along a direction determined by the mechanical force field acting on the particles, i.e., by the fluid dynamics of the system. In this case, the settling rate is ruled by the well-known Stokes law and is linearly proportional to the size of particles or flocs. Thus, the larger the flocs, the higher the settling rate and recovery yields. This is the reason why a flocculation step aimed to promote microalgae aggregation and floc size enlargement often precedes the harvesting one.

It is thus apparent that the knowledge of cells/flocs size distribution of the microalgal suspension is crucial when simulating, designing, or controlling the above processes. In this view, some works have been devoted to developing PBE models, that permit the assessment of the evolution of microalgae (or microalgae aggregates) size during the steps of flocculation and harvesting.

5.1.1. PBEs for modelling microalgae flocculation

In the microalgae industry, flocculation can be applied as the first of a two-step process for microalgae harvesting. Flocculants are chemicals added to neutralize negative charges on the cell surface, thus favouring cell aggregation [96]. The amount of chemicals to use increases with decreasing cell size since the surface-to-volume ratio becomes larger when cells become smaller. Moreover, the operating conditions usually involve force-fields applied to the suspension of microalgae, whose effect can depend on particle size, as in the case of differential settling, Brownian motion, or fluid share. Hence, one of the main variables affecting the flocculation process of a microalgal suspension is cell size [97,98]. Therefore, the general PBE adopted to describe microalgae flocculation is typically written by using the floc-volume, v, as an internal coordinate rather than the mass, m (Eq. (29)).

Actually, few works have been so far presented in the literature dealing with the use of PBEs for simulating microalgae flocculation. Some of them focus on the quantitative description of flocs size overshoot during prolonged microalgae flocculation [99,100], while some others deal with the interactive effects of fluid dynamics with the process when not-ideal force fields are acting inside the flocculation device [101]. PBEs have also been proposed to optimize and design a process where flocculation and sedimentation occur simultaneously. Indeed, such a model permits the evaluation of the settling time, the flocculant concentration and the tank size that maximize harvesting efficiency [22]. Finally, PBEs have also been used in non-industrial frameworks such as the assessment of the effect of microalgae flocculation on Suspended Particulate Matters (SPMs) formation in north European coastal areas [102]. Therefore, despite the high potential of PBEs, still few works have been presented in the literature aimed to exploit this mathematical tool to optimize the microalgal flocculation process. Accordingly, room for research activity exists in this sector. In what follows, a brief

Table 4
Comparison of main harvesting methods for algae [94,95].

Method	Post harvest concentration	Recovery yields	Major benefits	Major limitations
Centrifugation	12–22 wt%	> 90%	Reliable, high solids conc.	Energy-intensive, high cost
Membrane filtration	5–27 wt%	70–90%	Reliable, high solids conc.	Membrane fouling, high cost
Gravity sedimentation	0.5–3 wt%	10–90%	Low cost	Slow, unreliable
Dissolved air flotation	3–6 wt%	50–90%	Proven at large scale	Flocculants usually required
Electrocoagulation	Up to 60%	Up to 90%	Low dosage for coagulants, cost comparable with other technologies	Increased metal concentration, low technology readiness level

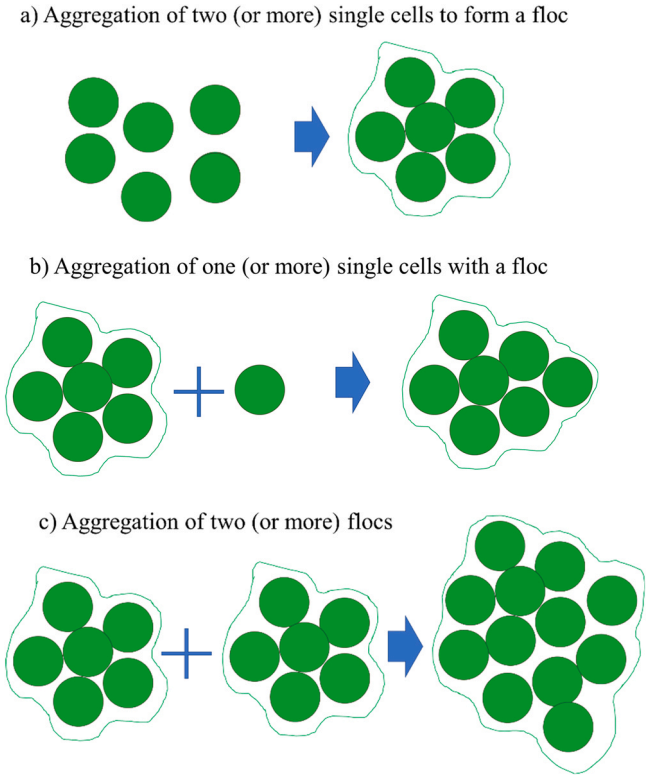

Fig. 6. Schematic representation of the main possible aggregation mechanisms of microalgae cells.

discussion about the mathematical form of PBEs in flocculation is reported.

5.1.2. Mathematical formulation of PBEs for simulating microalgal flocculation

The growth-related birth and death terms are usually neglected in the PBE model formulation because the characteristic times of growth and death are usually sufficiently lower than the harvesting time. The term *aggregation* identifies the formation of a floc starting from smaller entities which can be either smaller single cells or smaller flocs in different combinations as shown in Fig. 6. The term *breakage* is used to quantify the formation of flocs or single-cell entities due to breakage of a larger floc (Fig. 7). Hence, the size term in single-stage PBEs usually refers to generic particle size, and not specifically to cell size as in the case of growth-related PBE. In Eq. (29), $B_a(v, t)$ and $B_b(v, t)$ are the birth terms due to aggregation and breakage for a particle of size v respectively, and correspondingly $D_a(v, t)$ and $D_b(v, t)$are the death terms due to aggregation and breakage [103,104]:

$$\frac{\partial \psi(v, t)}{\partial t} = B_a(v, t) - D_a(v, t) + B_b(v, t) - D_b(v, t) \tag{26}$$

Birth of flocs of volume v by aggregation can be achieved when two smaller particles of generic sizes u and $v - u$ combine, resulting in the formation of a floc having volume just equal to v. In this case, the birth term is typically expressed by the following general formulation:

$$B_a(v, t) = \frac{1}{2}\int_0^v \beta_a(u, v - u)\, \psi(u, t)\, \psi(v - u, t)\, du \tag{27}$$

Where the symbol $\beta_a(u, v - u)$ refers to the *aggregation rate*, which is the product of the aggregation collision efficiency $\alpha_a(u, v - u)$and the frequency $\eta_a(u, v - u)$.

Aggregation phenomena can cause the disappearance of flocs of volume v when they aggregate with other particles of volume u to produce a floc of size larger than v, i.e. $v + u$. By applying a similar approach to the case of birth for mitosis, the death term can be thus written as follows:

$$D_a(v, t) = \int_0^\infty \beta_a(u, v)\, \psi(u, t)\, \psi(v, t)\, du \tag{28}$$

It should be noted that the adopted formulation contemplates only binary aggregation, i.e. the cases where aggregation involves two single cells, a cell and floc or two flocs.

Eqs. (30)-(31) consider aggregation as a global second-order kinetic event as demonstrated by the multiplicative term for the two particles densities with volume u and $v - u$ respectively. The disappearance of cell flocs belonging to the class size v can be due to the breakage of the floc, and Eq. (32) mathematically expresses the death rate due to this phenomenon:

$$D_b(v, t) = \beta_b(v, t)\, \psi(v, t) \tag{29}$$

In Eq. (32), $\beta_b(v, t)$represents the breakage rate, i.e., the frequency at which the particles break. Breakage of particles with volume w larger than v can result, with a certain probability, in the production of particles with size v. The symbol B_b in Eq. (33) represents the birth term describing the breakage of particles with size w which forms particles with size v.

$$B_b(v, t) = \int_v^\infty \beta_b(w, t)\, p(w, v)\, \psi(w, t)\, dw \tag{30}$$

where $p(w, v)$ is a partition function quantifying the probability that the breakage of a larger particle w could give rise to a particle of size equal to v.

5.1.2.1. Mathematical formulation of the aggregation rate. As mentioned above, the aggregation rate $\beta_{a,i}$ due to the generic i^{th} mechanism can be broadly defined as the product of the collision efficiency $\alpha_{a,i}$, and the collision frequency$\eta_{a,i}$, that is:

$$\beta_{a,i} = \alpha_{a,i}\, \eta_{a,i} \tag{31}$$

All the works dealing with the application of PBEs to simulate microalgae flocculation assume that the various mechanisms are contributing to aggregation overlay linearly [105]. Accordingly, the

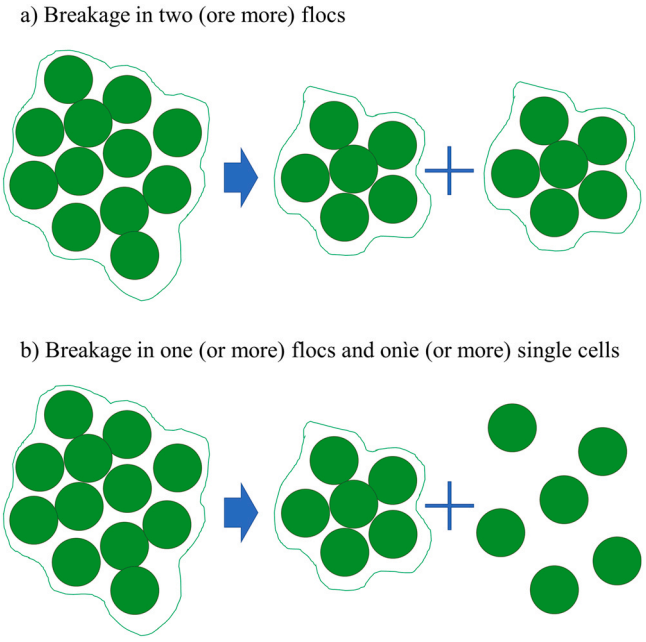

Fig. 7. Schematic representation of the main possible breakage mechanisms of microalgae flocs.

total aggregation rate is evaluated as the sum of the rates $\beta_{a,i}$ extended to all the n mechanisms considered (Eq. 35).

$$\beta_a = \sum_{i=1}^{n} \beta_{a,i} = \sum_{i=1}^{n} \alpha_{a,i}\eta_{a,i} \tag{32}$$

The collision efficiency $\alpha_{a,i}$ can be seen as the probability that two colliding cells do aggregate. To better distinguish among the factors influencing the collision efficiency, Schmideder [106] separated the physicochemical and the hydrodynamic effects.

In PBEs describing microalgae flocculation, the physicochemical effects are determined by the surface properties of colliding cells and specifically by the charge distribution as well as by the colloidal characteristics of particles [100]. However, in some works [102] the collision efficiency is represented by an adjustable parameter, while in some others [22,101] it is set equal to 1, thus assuming that all collisions lead to the formation of new flocs (aggregates). This is typically the case when flocculants are employed. These reduce attraction/repulsion forces and favour the collision between the particles (cells or flocs), thus justifying a collision efficiency equal to 1.

Instead, the hydrodynamic effect accounts for the action of the flow field around colliding particles which influences their tendency to create an aggregate. Such an effect has been taken into account in the model proposed by Schmideder et al. [106] to simulate microalgae flotation.

As mentioned above, the aggregation rate also depends on the collision frequency, which can, in turn, be affected by different mechanisms such as fluid shear, Brownian motion and differential settling [22,100–102]. The shear-induced collision frequency is usually described by functions similar to the one proposed by Smoluchowski [107], which involves the shear rate G and the third power of the sum of the colliding particle diameters. Two examples of the application of such an approach to the case of microalgae flocculation are provided in the models by Golzarijalal et al. [101] and Salim et al. [22] that assume particles to have a spherical shape, thus arriving at the aggregation rate reported in Eq. (36):

$$\beta_{i,j}^{a} = K\, G\, (d_i + d_j)^3 \tag{33}$$

Here K is a constant whose value was obtained by fitting to experimental data whiled_i and d_j are the diameters of colliding particles i and j, respectively. The model developed by Golzarijalal et al. [101] was successfully compared to experimental data obtained with *Chlorella sp.* in terms of flocs distribution at the end of the flocculation process as well as in terms of recovery efficiency evolution during settling. The model by Salim et al. [22] was successfully validated (specifically at late process time) by comparison with optical density experimental data obtained from flocculation/sedimentation of *Ettlia texensis*.

In other works, the aggregation rate is formulated starting from the more realistic assumption that particles and aggregates have an irregular shape and are permeable to the homogeneous phase [105]. In the latter case, a more complex fractal description is adopted wherein the aggregate mass, m, is related to the fractal dimension, d_f, and the characteristic collision length, l, by a relationship of the type $m \propto l^{d_f}$ [105].

Among the works adopting such an approach, it is worth mentioning the one by Sadegh-Vaziri et al. [100], who, by starting from the presumption that shear and Brownian motion are the main mechanisms affecting flocculation of microalgae and considering the mass of aggregate to be a function of the radius of gyration $R_p$and of the fractal dimension d_f, proposed the following expression for the aggregation rate:

$$\beta_a(m, m') = 1.3\, G\, R_p^3 \left(m^{\frac{1}{d_f}} + m'^{\frac{1}{d_f}}\right)^3 + \frac{2k_B T}{3\mu}\frac{(m^{\frac{1}{d_f}} + m'^{\frac{1}{d_f}})^2}{(mm')^{\frac{1}{d_f}}} \tag{34}$$

where k_B is the Boltzmann constant, T is the temperature and $\mu$the viscosity of the fluid. The latter ones are taken into account in Eq. (37) since Brownian motion was assumed to be among the main phenomena affecting aggregation. Accordingly, in the model presented in [91], the aggregation rate is proportional to the temperature, whose increase promotes the random particle motion. At the same time, it is inversely related to the fluid viscosity μ since viscous fluids tend to slow down the motion of particles. The model was successfully validated by comparing the experimental data of the mean aggregate size, fractal dimension, and radius of gyration with the corresponding model results. As seen in Figure 8b, the model allowed to capture well the overshoot phenomena taking place during flocculation. Accordingly, it represents a valuable tool for designing and optimising the microalgae flocculation process.

Shen et al. [93] proposed a similar approach, describing the collision radius of microalgae or their aggregates using a fractal dimension. However, in this case, a third mechanism was considered to affect microalgae flocculation: differential settling, which consists of particles submerged in a fluid following the direction of the applied force field, such as gravity or centrifugal forces, involved in the flocculation process. Shen et al. [102] considered the differential settling aggregation rate to be proportional both to the square sum of the particles fractal size, and to the difference between the settling velocities $w_{s,i}$ of the particles as reported in Eq. (38):

$$\beta_{i,j}^{a} = \frac{1}{6} G\, (d_i + d_j)^3 + \frac{\pi}{4} (d_i + d_j)^2\, |w_{s,i} - w_{s,j}| + \frac{2k_B T}{3\mu}\left(\frac{1}{d_i} + \frac{1}{d_j}\right)(d_i + d_j) \tag{35}$$

where the settling velocities are usually described by the Stokes law or modified Stokes laws to count deviations from the regular law behavior in case of large particles.

The model developed by Shen et al. [102] was mainly used to simulate the mass fraction and the size/time-evolution of different flocs size classes (Mega-flocs, macro-flocs, and micro-flocs) in a north European costal system, which is likely to be influenced by algae bloom in specific periods of the year. So, the model was successfully compared to seasonal data of mean floc size and settling velocity, taking into account the time evolution of the along-shore velocity.

5.1.2.2. Mathematical formulation of the breakage rate. During the flocculation process, the flocs can also break apart, generating smaller particles/aggregates. Unfortunately, there are no first-principles theories about the breakage process, and consequently, PBEs usually adopt empirical relations containing tunable parameters to describe the process. As shown in Eq. (32), the sink term of the breakage process is represented by first-order kinetics, and thus it is described as the particle number distribution multiplied by a constant. When considering applications to the case of microalgae flocculation, the breakage rate is generally quantified by the power law of the local dissipation energy and of the share rate (G). Sadegh-Vaziri and Babler [99], by adopting an approach typically used for brittle particles, proposed an empirical formulation of breakage frequency which depends on the shear rate through the local dissipation energy ε, and the critical dissipation energy ε_{cr} as shown in the following equation:

$$\ln\left(\frac{\beta_b}{G}\right) = \begin{cases} -0.457x_b - 2.8775 & for \quad x_b \le -2 \\ -0.00104x_b^4 - 0.02284x_b^3 - 0.149x_b^2 - 0.8138x_b - 3.16 & for \quad x_b \ge -2 \end{cases} \tag{36}$$

Here $x_b = \ln(\varepsilon_{cr}/\varepsilon) = Cm^{-2/(d_f p1)}$, C is an adjustable coefficient related to particle strength, $d_f$the fractal dimension, $p_1$an adjustable

parameter, and m the mass class size. As mentioned above, such a representation of the breakage kernel implies fragile particle behavior, meaning that when the particle approaches a critical value for the dissipation energy, it tends to break suddenly.

Shen et al. [102] proposed a breakage frequency inversely proportional to the square root of the floc strength F_y which was, in turn, assumed to linearly decrease with the floc size D_{Fi}. The breakage frequency proposed by Shen et al. [102] is reported in Eq. (40) and was assumed to increase with the floc size, which, in turn, was estimated through the relative fractal size $\left(\frac{D_{Fi}-D_P}{D_P}\right)^{3-nf}$ where nf is the fractal dimension, and D_P is the diameter of the elementary particles, i.e. microalgae cells:

$$\beta_i^b = E_b\, G \left(\frac{D_{Fi}-D_P}{D_P}\right)^{3-nf} \left(\frac{\mu G}{F_y/D_{Fi}^2}\right)^{\frac{1}{2}} \quad (i = 1, 2) \tag{37}$$

In Eq. (40), E_b represents an adjustable parameter, G is the shear rate and $\mu$the viscosity of the fluid where cells and flocs are submerged.

Golzarijalal et al. [101] presented the following power law to describe the breakage rate of microalgae flocs as a function of the shear rate:

$$\beta_i^b = c_2\, G^{c_3}\, \vartheta_i^{\delta} \tag{38}$$

where G is the shear rate, ϑ_i the i^{th} particle size while c_2, c_3, δ are adjustable parameters.

5.1.2.3. Mathematical formulation of partition functions. The aggregates undergoing breakage generate particles that need a size distribution specification. The aforementioned phenomenon is usually addressed by considering a specific partition function. In the field of microalgae flocculation, the most simple partition function expresses the size of the fragmented particles as the ratio between the breaking particle and the newly formed ones. A subcategory of this approach is the so-called equipartitioned binary fission, where the ratio above is equal to two, meaning that the particle divides into two alike particles [101]. A symmetric binary partitioning breakage function for particles of mass m' dividing into particles of mass m was adopted by Sadegh-Vaziri et al. [100] and it is shown in Eq. (42) where b is an adjustable parameter.

$$g(m, m') = (b+1)\,\frac{2}{m'}\left(-\left|\frac{2m}{m'}\right| + 1\right)^b \tag{39}$$

No further examples of partition functions associated with flocs breakage could be found in the literature as far as microalgae-based processes are concerned.

5.2. PBEs for modelling microalgae harvesting by gravity settling or centrifugation

As mentioned above, harvesting is one of the most expensive section of microalgae-based processes which are strongly size-dependent, and among the others, sedimentation and centrifugation are two of the most widespread operations to harvest microalgae cells. The size dependence of the operation makes PBEs potentially useful during the design and optimization of the equipment. The generic equation uses a continuous term along with the spatial distance travelled by the particles (h), and the cell growth does not represent a relevant term in the process. Therefore, according to Lee et al. [108], the PBE for describing microalgae harvesting assumes the general form reported in Eq. (43):

$$\frac{\partial \psi(t, z, d)}{\partial t} = \frac{\partial [v_h(t, h, d)\, \psi(t, h, d)]}{\partial h} \tag{40}$$

According to the authors, the expression of the velocity $v_h(t, h, d)$ depends on the position h, and the cell size d. A particle settling in a fluid usually follows the direction of the field force generating the settling, and its velocity increases until it reaches its terminal value when a steady state is achieved in terms of the motion. For dilute solutions, the Stokes law reported in Eq. (44) holds true, thus permitting to evaluate the terminal velocity as a function of particle and fluid densities ρ_p and ρ_f, gravitational acceleration g, particle size d, and fluid viscosity μ:

$$v_{t,s} = \frac{(\rho_p - \rho_f)\, g\, d^2}{18\mu} \tag{41}$$

Such an equation was adopted by Lee et al. [108] to quantitatively describe microalgae settling in a natural gravitational force field. However, the same authors simulated also harvesting of microalgae by centrifugation by adopting an adaptation of the Stokes law to the case where the force field was produced by a centrifugal motion of the fluid, i.e.:

$$v_{t,c} = \frac{(\rho_p - \rho_f)\, r_c\, \omega^2\, d^2}{18\mu} \tag{42}$$

where $r_c$is the radius of the centrifuge and ω the centrifuge rotational speed.

The application of the PBE considers that the terminal velocity is immediately reached so that it can be expressed as a function of the cell size. In Lee et al. [108], the density of the cells was considered as size specific, with values varying from 1044 to 1137 kg m^{-3} in a cell size range between 2.75 and 9 µm.

Model results were compared to experimental data obtained when considering both sedimentation and centrifugation cases. At the end of the harvesting process, the experimental data coming both from settling and centrifugation were compared with the model outputs. It is worth noting that the model accounting for a variable cell density could better predict the data compared with the model developed under the assumption of constant cell density.

A PBM framework, like the one reported in Eq. (43), was developed for the evaluation of the cellular density during the harvesting in case of sedimentation and centrifugation. The model combined with a specific experimental procedure provided a tool that could help in the development of downstream separation techniques. In this work, cell size and the cycle stage of the cell growth are potentially interconnected with the cellular density itself. Having different density, the effects of the force field acting on the cells can have different impact when it comes to sedimentation or centrifugation [109].

5.3. PBEs for modelling microalgae harvesting by microfiltration

Microfiltration is a harvesting alternative to sedimentation and centrifugation. During microfiltration, the solution containing particles is passed through a filter with a mesh dimension usually close to the typical size of microalgae cells, i.e. from 1 to 2–10 µm. To the best of our knowledge, only one paper [110] can be found in the literature where the following PBE is used to simulate microalgae filtration:

$$\frac{\partial \psi(t, h, d)}{\partial t} = v\frac{\partial [1 - \Phi(h, d)]\, \psi(t, h, d)]}{\partial h} \tag{43}$$

It can be seen that a convective term along the h axis (parallel to the motion of the bulk fluid) is adopted in the PBE to account for the fact that the motion of microalgae cells along the porous medium (filter) is hindered as their size increases. The term Φ, which is a function of the cells size distribution, accounts for the fact that the

convective velocity of the cells should decrease within the filter as much as their size increases. Therefore, in discrete terms, the filtration coefficient Φ assumed different values for each size class of the cells. Lee et al. [110] obtained the value of Φ as a function of the cell size d by fitting suitable experimental data obtained with *Chlorella vulgaris.* This way the authors achieved the non-trivial result that the pattern of $\Phi(d)$ became convex thus indicating that small and large cells are preferred for filtration in large pores filters rather than cells of intermediate size [110]. This is probably because very small cells tend to form large aggregates that are more efficiently captured by the filter. Moreover, electrostatic phenomena leading small cells to be captured by the filter probably took place in large pores. According to the authors, such an outcome (i.e. the convexity of $\Phi(d)$)needs a deeper investigation to establish a direct relation between the filtration and the electrostatic attraction in this case.

Derived size-specific filtration coefficients of microalgae were obtained by calibrating the model with the experimental data derived from *Chlorella sp.* filtering. Specifically, the model helps to identify different patterns in the filtration coefficient depending on the filter pore size.

5.4. Use of PBEs for the optimization of the cell disruption section

The microalgae industry mainly focuses on the sustainable production of added-value chemicals. Such compounds are usually intracellular; therefore, an extraction process is required to separate these products from others [111]. Extraction is usually high-energy demanding, and strategies to reduce its cost should be developed. Several possible cell disruption treatments have been proposed so far. For all of them, the efficiency is dependent on cell size. Indeed, the larger microalgae cells are, the more easily to be disrupted as compared to smaller ones [29,30]. As a result, the simulations of these processes by employing PBEs could contribute to their improvement. Nevertheless, to our knowledge, only one paper applied PBEs to describe cell disruption [29], i.e. mechanical disruption. Cell size is not the only parameter to be taken into account. Other biological features also have an impact, as the composition of the cell wall, which can change remarkably depending on the microalgal species [25]. A classic discretized formulation of PBEs adopted for bead milling disruption of a microalgae cell population is shown in Eq. (47), and it was specifically used to describe the different size-dependent phenomena which can affect the cell size class w_i [29,30]:

$$\frac{d\mathrm{w}_i(t)}{dt} = -S_j\, w_i(t) + \sum_{j=1}^{i-1} b_{i,j}\, S_j\, w_j(t) \tag{44}$$

By using this equation, some authors inferred that the shear effect prevails in the disruption of smaller particles and compression effects in larger particles [29,30]. As in flocculation breakage processes, the breakage due to bead milling can be represented by a *stress* model, which is a function of the overall stress applied on the cells, strictly related to the cell size. Zinkoné et al. [30] tried to extend the effect of the disruption variables to the efficiency of the main products extraction from microalgae biomass. The model proposed by Pan et al. [29] was used to fit experimental data coming from *Nannochloropsis sp.*

6. Concluding remarks and future perspectives

PBE models have been proposed to optimize different operating steps involved in the microalgae process industry. Operating steps that could greatly benefit from PBE application are microalgae cultivation, harvesting, disruption and extraction.

PBE models have been formulated to analyze the impact of cell cycle progression, multiple fission and lysis on population growth dynamics. Integrating the description of these phenomena into the modeling of microalgae growth through PBEs allowed the explaination of complex cultivation dynamics, such as the onset of transient oscillations and the synchronization of microalgae cells in response to nutrient availability fluctuations, which are determined by cell-to-cell heterogeneity and cannot be reproduced by traditional unsegregated models. Furthermore, the use of PBE models was demonstrated to prevent the erroneous estimation of average specific growth rate, which is determined if an average biomass concentration is used, as specific growth rate is nonlinearly dependent on nutrient concentrations.

Downstream processes (harvesting and cell disruption) always include size/mass dependent treatments, and the use of PBE highlighted how different particle/cells sizes behave differently when exposed to the same operating conditions. PBEs have been used to describe the effect that different particle size can display on the formation of larger particles and on settling and centrifugation.

Classical formulations of PBEs have even been applied to describe mechanical cell disruption of cells.

Nevertheless, the potential of PBE models to analyze and simulate microalgae growth dynamics has not fully exploited yet. Although it is extensively recognized that single cell growth dynamics can be hardly described based on the knowledge of a unique internal variable, univariate PBE models were typically formulated, where the state of cells was identified by either the size/mass or the position through the cell cycle, while only few studies were found describing the cell state by multiple internal variables. Even in this latter case, only the mass and/or the position within the cell cycle were used as internal variables, while scarce efforts were devoted to developing PBE models predicting the distribution of biomass fractions (e.g. lipids, carbohydrates, proteins) within the cell population.

These limitations can be attributed to the increasing computational difficulties that are introduced with increasing the number of internal variables and to the lack of quantitative experimental data about the biochemical composition of single cells. However, the increasing availability of computational resources combined with the development of efficient computational solution schemes [112,113] and the rapid advancement in the development of analytical methods for single-cell analysis recorded over the past few years could help overcome these limitations [16,114]. Analytical techniques have been continuously improved, allowing the collection of quantitative data on intracellular lipids, starch, and protein as well as the growth rate. In addition, such experimental data can be used to gain further insights into the mechanisms driving the occurrence of phenotypic heterogeneity (i.e., the differentiation of isogenic cells in the absence of mutations [18]) and their effect on the dynamic behavior of microalgae. Cells with different specific growth rates or different fractions of accumulated reserve materials may, for example, exhibit different resistances to conditions like nutrient starvation [85] or the presence of antimicrobial compounds [115]. Even random variations in the metabolism can determine the cellular fate under variable nutrient supply [116]. In this framework, PBE formulations tracking the distribution of biomass composition variables could be integrated with mathematical models describing the ability of single cells to switch between different metabolic states in response to random fluctuations [89,117,118]. By taking advantage of experimental data of biochemical composition distribution becoming increasingly available, the resulting integrated models can be used to validate the mechanisms proposed for the switching, and subsequently implemented to predict the heterogeneous response recorded under time-varying environmental conditions.

CRediT authorship contribution statement

Alessandro Usai: Conceptualization, Investigation, Methodology, Data curation, Writing – original draft, Writing – review & editing,

Visualization. **Constantinos Theodoropoulos:** Investigation, Writing – review & editing. **Fabrizio Di Caprio:** Investigation, Writing – review & editing. **Pietro Altimari:**, Investigation, Writing – review & editing. **Giacomo Cao:** Investigation, Writing – review & editing. **Alessandro Concas:** Supervision, Methodology, Conceptualization, Investigation, Data curation, Writing – original draft, Writing – review & editing, Visualization.

Declaration of Competing Interest

The authors declare that they have no known competing financial interests or personal relationships that could have appeared to influence the work reported in this paper.

References

[1] Concas A, Lutzu GA, Turgut Dunford N. Experiments and modeling of Komvophoron sp. Growth in hydraulic fracturing wastewater. Chem Eng J 2021. https://doi.org/10.1016/j.cej.2021.131299

[2] Concas A, Lutzu GA, Pisu M, Cao G. Experimental analysis and novel modeling of semi-batch photobioreactors operated with Chlorella vulgaris and fed with 100%(v/v) CO_2. Chem Eng J 2012;213:203–13. https://doi.org/10.1016/j.cej.2012.09.119

[3] Bekirogullari M, Figueroa-Torres GM, Pittman JK, Theodoropoulos C. Models of microalgal cultivation for added-value products - a review. Biotechnol Adv 2020;44:107609https://doi.org/10.1016/j.biotechadv.2020.107609

[4] Concas A, Lutzu GA, Pisu M, Cao G. On the feasibility of Pseudochloris wilhelmii cultivation in sea–wastewater mixtures: Modeling and experiments. J Environ Chem Eng 2019;7:103301.

[5] Concas A., Pisu M., Cao G. Mathematical modelling of Chlorella vulgaris growth in semi-batch photobioreactors fed with pure CO < inf > 2 < /inf > . vol. 32. 2013. https://doi.org/10.3303/CET1332171.

[6] Tong ZX, Li MJ, Yan JJ, Gu ZL. A theoretical analysis of the hydrodynamic influence on the growth of microalgae in the photobioreactors with simple growth kinetics. Int J Heat Mass Transf 2020. https://doi.org/10.1016/j.ijheatmasstransfer.2020.119986

[7] Pires JCM, Alvim-Ferraz MCM, Martins FG. Photobioreactor design for microalgae production through computational fluid dynamics: a review. Renew Sustain Energy Rev 2017. https://doi.org/10.1016/j.rser.2017.05.064

[8] Mairet F, Bernard O, Masci P, Lacour T, Sciandra A. Modelling neutral lipid production by the microalga Isochrysis aff. galbana under nitrogen limitation. Bioresour Technol 2011;102:142–9.

[9] Bernard O. Hurdles and challenges for modelling and control of microalgae for CO 2 mitigation and biofuel production. J Process Control 2011;21:1378–89.

[10] Packer A, Li Y, Andersen T, Hu Q, Kuang Y, Sommerfeld M. Growth and neutral lipid synthesis in green microalgae: a mathematical model. Bioresour Technol 2011;102:111–7.

[11] Concas A, Steriti A, Pisu M, Cao G. Comprehensive modeling and investigation of the effect of iron on the growth rate and lipid accumulation of Chlorella vulgaris cultured in batch photobioreactors. Bioresour Technol 2014;153:340–50. https://doi.org/10.1016/j.biortech.2013.11.085

[12] Figueroa-Torres GM, Pittman JK, Theodoropoulos C. Kinetic modelling of starch and lipid formation during mixotrophic, nutrient-limited microalgal growth. Bioresour Technol 2017;241:868–78. https://doi.org/10.1016/j.biortech.2017.05.177

[13] Bekirogullari M, Fragkopoulos IS, Pittman JK, Theodoropoulos C. Production of lipid-based fuels and chemicals from microalgae: an integrated experimental and model-based optimization study. Algal Res 2017;23:78–87. https://doi.org/10.1016/J.ALGAL.2016.12.015

[14] Figueroa-Torres GM, Pittman JK, Theodoropoulos C. A highly productive mixotrophic fed-batch strategy for enhanced microalgal cultivation. Sustain Energy Fuels 2022;6:2771–82. https://doi.org/10.1039/d2se00124a

[15] Luzi G, McHardy C. Modeling and simulation of photobioreactors with computational fluid dynamics—a comprehensive review. Energies 2022;15:3966.

[16] He Y, Zhang P, Huang S, Wang T, Ji Y, Xu J. Label-free, simultaneous quantification of starch, protein and triacylglycerol in single microalgal cells. Biotechnol Biofuels 2017;10:1–18. https://doi.org/10.1186/S13068-017-0967-X/FIGURES/6

[17] Di Caprio F, Pagnanelli F, Wijffels RH, Van der Veen D. Quantification of Tetradesmus obliquus (Chlorophyceae) cell size and lipid content heterogeneity at single-cell level. J Phycol 2018;54:187–97. https://doi.org/10.1111/jpy.12610

[18] Damodaran SP, Eberhard S, Boitard L, Rodriguez JG, Wang Y, Bremond N, et al. A millifluidic study of cell-to-cell heterogeneity in growth-rate and cell-division capability in populations of isogenic cells of chlamydomonas reinhardtii. PLoS One 2015;10:e0118987https://doi.org/10.1371/JOURNAL.PONE.0118987

[19] Concas A, Pisu M, Cao G. A novel mathematical model to simulate the size-structured growth of microalgae strains dividing by multiple fission. Chem Eng J 2016;287:252–68. https://doi.org/10.1016/j.cej.2015.11.021

[20] Kandilian R, Lee E, Pilon L. Radiation and optical properties of Nannochloropsis oculata grown under different irradiances and spectra. Bioresour Technol 2013;137:63–73.

[21] Yap BHJ, Crawford SA, Dagastine RR, Scales PJ, Martin GJO. Nitrogen deprivation of microalgae: effect on cell size, cell wall thickness, cell strength, and resistance to mechanical disruption. J Ind Microbiol Biotechnol 2016. https://doi.org/10.1007/s10295-016-1848-1

[22] Salim S, Gilissen L, Rinzema A, Vermuë MH, Wijffels RH. Modeling microalgal flocculation and sedimentation. Bioresour Technol 2013;144:602–7.

[23] Concas A, Pisu M, Cao G. Mathematical modeling of the size-structured growth of microalgae dividing by multiple fission. Chem Eng Trans 2019;74:199–204. https://doi.org/10.3303/CET1974034

[24] Gerardo ML, Zanain MA, Lovitt RW. Pilot-scale cross-flow microfiltration of Chlorella minutissima: a theoretical assessment of the operational parameters on energy consumption. Chem Eng J 2015;280:505–13.

[25] Günerken E, D'Hondt E, Eppink MHMM, Garcia-Gonzalez L, Elst K, Wijffels RH. Cell disruption for microalgae biorefineries. Biotechnol Adv 2015;33:243–60. https://doi.org/10.1016/j.biotechadv.2015.01.008

[26] Concas A, Pisu M, Cao G. Disruption of microalgal cells for lipid extraction through Fenton reaction: Modeling of experiments and remarks on its effect on lipids composition. Chem Eng J 2015:263. https://doi.org/10.1016/j.cej.2014.11.012

[27] Steriti A, Rossi R, Concas A, Cao G. A novel cell disruption technique to enhance lipid extraction from microalgae. Bioresour Technol 2014;164:70–7. https://doi.org/10.1016/j.biortech.2014.04.056

[28] Postma PR, Miron TL, Olivieri G, Barbosa MJ, Wijffels RH, Eppink MHM. Mild disintegration of the green microalgae Chlorella vulgaris using bead milling. Bioresour Technol 2015;184:297–304.

[29] Pan Z, Huang Y, Wang Y, Wu Z. Disintegration of Nannochloropsis sp. cells in an improved turbine bead mill. Bioresour Technol 2017;245:641–8. https://doi.org/10.1016/j.biortech.2017.08.146

[30] Zinkoné TR, Gifuni I, Lavenant L, Pruvost J, Marchal L. Bead milling disruption kinetics of microalgae: Process modeling, optimization and application to biomolecules recovery from Chlorella sorokiniana. Bioresour Technol 2018;267:458–65. https://doi.org/10.1016/j.biortech.2018.07.080

[31] Sandmann M, Schafberg M, Lippold M, Rohn S. Analysis of population structures of the microalga Acutodesmus obliquus during lipid production using multi-dimensional single-cell analysis. Sci Rep 2018 81 2018;8:1–9. https://doi.org/10.1038/s41598-018-24638-y

[32] Rioboo C, O'Connor JE, Prado R, Herrero C, Cid Á. Cell proliferation alterations in Chlorella cells under stress conditions. Aquat Toxicol 2009;94:229–37.

[33] Ting YP, Lawson F, Prince IG. The influence of cadmium and zinc on the cell size distribution of the alga Chlorella vulgaris. Chem Eng J 1991;47:B23–34.

[34] Mantzaris NV, Liou J-JJ, Daoutidis P, Srienc F. Numerical solution of a mass structured cell population balance model in an environment of changing substrate concentration. J Biotechnol 1999;71:157–74. https://doi.org/10.1016/S0168-1656(99)00020-6

[35] Hlavová M, Vítová M, Bišová K. Synchronization of green algae by light and dark regimes for cell cycle and cell division studies. Methods Mol Biol 2016;vol. 1370:3–16. https://doi.org/10.1007/978-1-4939-3142-2_1

[36] Di Caprio F, Altimari P, Iaquaniello G, Toro L, Pagnanelli F. Heterotrophic cultivation of T. obliquus under non-axenic conditions by uncoupled supply of nitrogen and glucose. Biochem Eng J 2019;145:127–36. https://doi.org/10.1016/j.bej.2019.02.020

[37] Bišová KK, Zachleder V. Cell-cycle regulation in green algae dividing by multiple fission. J Exp Bot 2014;65:ert466. https://doi.org/10.1093/jxb/ert466

[38] Sporleder F., Borka Z., Solsvik J., Jakobsen H.A. On the population balance equation 2012.

[39] Hulburt HM, Katz S. Some problems in particle technology. A statistical mechanical formulatio. Chem Eng Sci 1964;19:555–74. https://doi.org/10.1016/0009-2509(64)85047-8

[40] Ramkrishna D. The status of population balances Doraiswami Ramkrishna. Rev Chem Eng 1985:49–95.

[41] Randolph ADD. A population balance for countable entities. Can J Chem Eng 1964;42:280–1. https://doi.org/10.1002/cjce.5450420612

[42] Jakobsen HA, Lindborg H, Dorao CA. Modeling of bubble column reactors: progress and limitations. Ind Eng Chem Res 2005;44:5107–51.

[43] Concas A, Pisu M, Cao G. Novel simulation model of the solar collector of BIOCOIL photobioreactors for CO_2 sequestration with microalgae. Chem Eng J 2010;157:297–303. https://doi.org/10.1016/j.cej.2009.10.059

[44] Millies M, Mewes D. Interfacial area density in bubbly flow. Chem Eng Process Process Intensif 1999;38:307–19. https://doi.org/10.1016/S0255-2701(99)00022-7

[45] Rigopoulos S. Population balance modelling of polydispersed particles in reactive flows. Prog Energy Combust Sci 2010;36:412–43. https://doi.org/10.1016/J.PECS.2009.12.001

[46] Ramkrishna D. Population Balances Theory and Applications to Particulate Systems Engineering. Elsevier; 2000.

[47] Randolph AD, Larson MA. Theory of Particulate Processes Analysis and Techniques of Continuous Crystallization. Elsevier; 1971. https://doi.org/10.1016/b978-0-12-579650-7.x5001-5

[48] Ramkrishna D, Singh MR. Population balance modeling: Current status and future prospects. Annu Rev Chem Biomol Eng 2014;5:123–46.

[49] Fredrickson AG, Mantzaris NV. A new set of population balance equations for microbial and cell cultures. Chem Eng Sci 2002;57:2265–78. https://doi.org/10.1016/S0009-2509(02)00116-1

[50] Mantzaris NV, Daoutidis P. Cell population balance modeling and control in continuous bioreactors. J Process Control 2004;14:775–84.

[51] Pisu M, Concas A, Cao G. A novel quantitative model of cell cycle progression based on cyclin-dependent kinases activity and population balances. Comput Biol Chem 2015;55:1–13. https://doi.org/10.1016/j.compbiolchem.2015.01.002
[52] Pisu M, Concas A, Cao G. Simulation models for stem cells differentiation. Chem Biochem Eng Q 2012;26:435–46.
[53] Pisu M, Concas A, Fadda S, Cincotti A, Cao G. A simulation model for stem cells differentiation into specialized cells of non-connective tissues. Comput Biol Chem 2008;32:338–44. https://doi.org/10.1016/j.compbiolchem.2008.06.001
[54] Srienc F. Cytometric data as the basis for rigorous models of cell population dynamics. J Biotechnol 1999;71:233–8. https://doi.org/10.1016/S0168-1656(99)00026-7
[55] Pahija E, Hui CW. A systematic study on the effects of dynamic environments on microalgae concentration. Algal Res 2019. https://doi.org/10.1016/j.algal.2019.101599
[56] Griffiths MJ, Garcin C, van Hille RP, Harrison STL. Interference by pigment in the estimation of microalgal biomass concentration by optical density. J Microbiol Methods 2011. https://doi.org/10.1016/j.mimet.2011.02.005
[57] Mancuso L, Liuzzo MI, Fadda S, Pisu M, Cincotti A, Arras M, et al. Experimental analysis and modelling of in vitro proliferation of mesenchymal stem cells. Cell Prolif 2009:42. https://doi.org/10.1111/j.1365-2184.2009.00626.x
[58] Bertucco A, Sforza E, Fiorenzato V, Strumendo M. Population balance modeling of a microalgal culture in photobioreactors: comparison between experiments and simulations. AIChE J 2015;61:2702–10. https://doi.org/10.1002/aic
[59] Usai A, Pittman J, Theodoropoulos C. A multiscale model approach for cell growth for lipids and pigments production by Haematococcus pluvialis under different environmental conditions. Comput Aided. Chem Eng 2019;46:1573–8. https://doi.org/10.1016/B978-0-12-818634-3.50263-0
[60] Cermak N, Becker JW, Knudsen SM, Chisholm SW, Manalis SR, Polz MF. Direct single-cell biomass estimates for marine bacteria via Archimedes' principle. ISME J 2017;11:825–8. https://doi.org/10.1038/ismej.2016.161
[61] Reinecke DL, Castillo-Flores A, Boussiba S, Zarka A. Polyploid polynuclear consecutive cell-cycle enables large genome-size in Haematococcus pluvialis. Algal Res 2018;33:456–61. https://doi.org/10.1016/J.ALGAL.2018.06.013
[62] Mancuso L, Liuzzo MII, Fadda S, Pisu M, Cincotti A, Arras M, et al. In vitro ovine articular chondrocyte proliferation: experiments and modelling. Cell Prolif 2010;43:310–20. https://doi.org/10.1111/j.1365-2184.2010.00676.x
[63] Mancuso L, Scanu M, Pisu M, Concas A, Cao G. Experimental analysis and modelling of in vitro HUVECs proliferation in the presence of various types of drugs. Cell Prolif 2010;43:617–28. https://doi.org/10.1111/j.1365-2184.2010.00711.x
[64] Pahija E, Liang Y, Hui CW. Determination of microalgae growth in different temperature condition using a population balance equation. Chem Eng Trans 2017;61:721–6. https://doi.org/10.3303/CET1761118
[65] Usai A, Pittman JK, Theodoropoulos C. A multiscale modelling approach for Haematococcus pluvialis cultivation under different environmental conditions. Biotechnol Rep 2022. https://doi.org/10.1016/j.btre.2022.e00771
[66] Altimari P, Pagnanelli F, Toro L. Application of structured population balance model for the numerical simulation of a continuous photobioreactor. Chem Eng Trans 2013;32:1027–32. https://doi.org/10.3303/CET1332172
[67] Lara GA, Moreno L, Ram\"\irez Y, Cisternas LA. Modeling an Airlift Reactor for the Growing of Microalgae. Open Chem Eng J 2018;12. 1874–1231.
[68] Pisu M, Lai N, Concas A, Cao G. A novel simulation model for engineered cartilage growth in static systems. Tissue Eng 2006;12:2311–20. https://doi.org/10.1089/ten.2006.12.2311
[69] Droop MR. 25 years of algal growth kinetics a personal view. Bot Mar 1983;26:99–112.
[70] Andrews JF. A mathematical model for the continuous culture of microorganisms utilizing inhibitory substrates. Biotechnol Bioeng 1968;10:707–23.
[71] Finkel Z, Irwin A, Schofield O. Resource limitation alters the 3/4 size scaling of metabolic rates in phytoplankton. Mar Ecol Prog Ser 2004;273:269–79. https://doi.org/10.3354/meps273269
[72] Aksnes DL, Egge JK. A theoretical model for nutrient uptake in phytoplankton. Mar Ecol Prog Ser Oldend 1991;70:65–72.
[73] Dao M. Reassessment of the cell surface area limitation to nutrient uptake in phytoplankton. Mar Ecol Prog Ser 2013;489:87–92. https://doi.org/10.3354/meps10434
[74] Mei Z-P, Finkel ZV, Irwin AJ. Light and nutrient availability affect the size-scaling of growth in phytoplankton. J Theor Biol 2009;259:582–8.
[75] Pahija E, Lee PY, Hui C-W. A revision of population balance equation applied to microalgae with birth, growth, and death. Process Integr Optim Sustain 2019;3:125–41. https://doi.org/10.1007/s41660-018-0059-9
[76] Travieso L, Hall DO, Rao KK, Benítez F, Sánchez E, Borja R. A helical tubular photobioreactor producing Spirulina in a semicontinuous mode. Int Biodeterior Biodegrad 2001. https://doi.org/10.1016/S0964-8305(01)00043-9
[77] Strumendo M, Arastoopour H. Solution of PBE by MOM in finite size domains. Chem Eng Sci 2008;63:2624–40. https://doi.org/10.1016/j.ces.2008.02.010
[78] Šetlík I, Zachleder V. The multiple fission cell reproductive patterns in algae. Microb Cell Cycle 1984:253–79.
[79] Yamamoto M, Nozaki H, Miyazawa Y, Koide T, Kawano S. Relationship between presence of a mother cell wall and speciation in the unicellular microalga *Nannochloris* (CHLOROPHYTA) [1]. J Phycol 2003;39:172–84. https://doi.org/10.1046/j.1529-8817.2003.02052.x
[80] Rading MM, Engel TA, Lipowsky R, Valleriani A. Stationary size distributions of growing cells with binary and multiple cell division. J Stat Phys 2011;145:1–22.
[81] Pahija E, Hui CW. A practical approach for modelling the growth of microalgae with population balance equation. New Biotechnol 2021. https://doi.org/10.1016/j.nbt.2021.01.001
[82] Concas A, Malavasi V, Costelli C, Fadda P, Pisu M, Cao G, et al. Autotrophic growth and lipid production of Chlorella sorokiniana in lab batch and BIOCOIL photobioreactors: experiments and modeling. Bioresour Technol 2016;211:327–38. https://doi.org/10.1016/j.biortech.2016.03.089
[83] Zachleder V., Vítová M. The cell cycle of microalgae, 2016. https://doi.org/10.1007/978–3-319–24945-2.
[84] Ivanov IN, Vítová M, Bišová K. Growth and the cell cycle in green algae dividing by multiple fission. Folia Microbiol 2019;64:663–72. https://doi.org/10.1007/s12223-019-00741-z
[85] Di Caprio F, Tocca GP, Stoller M, Pagnanelli F, Altimari P. Control of bacterial contamination in microalgae cultures integrated with wastewater treatment by applying feast and famine conditions. J Environ Chem Eng 2022;10:108262https://doi.org/10.1016/J.JECE.2022.108262
[86] Pascual M, Caswell H. From the cell cycle to population cycles in phytoplankton-nutrient interactions. Ecology 1997;78:897–912. https://doi.org/10.1890/0012-9658(1997)078[0897:FTCCTP]2.0.CO;2
[87] Massie TM, Blasius B, Weithoff G, Gaedke U, Fussmann GF. Cycles, phase synchronization, and entrainment in single-species phytoplankton populations. Proc Natl Acad Sci USA 2010;107:4236–41. https://doi.org/10.1073/pnas.0908725107
[88] Di Caprio F. Cultivation processes to select microorganisms with high accumulation ability. Biotechnol Adv 2021;49:107740https://doi.org/10.1016/J.BIOTECHADV.2021.107740
[89] Schreiber F, Littmann S, Lavik G, Escrig S, Meibom A, Kuypers MMM, et al. Phenotypic heterogeneity driven by nutrient limitation promotes growth in fluctuating environments. Nat Microbiol 2016:1. https://doi.org/10.1038/nmicrobiol.2016.55
[90] Mairet F, Baron R. A physiologically structured equation to consider quota heterogeneity in the droop model. IFAC-Pap 2019;vol. 52:275–80. https://doi.org/10.1016/j.ifacol.2019.12.270
[91] Di Caprio F. A fattening factor to quantify the accumulation ability of microorganisms under N-starvation. N Biotechnology 2022;66:70–8. https://doi.org/10.1016/J.NBT.2021.04.001
[92] Modenes AN, Zaharieva M, Najdenski H. Modeling and Technoeconomic Analysis of Algae for Bioenergy and Coproducts. Elsevier B.V; 2017. https://doi.org/10.1016/B978-0-444-63784-0.00011-4
[93] Jackson G. Living at micro scale: the unexpected physics of being small. Oceanography 2009. https://doi.org/10.5670/oceanog.2009.91
[94] Concas A, Pisu M, Cao G. Engineering aspects related to the use of microalgae for biofuel production and CO_2 capture from flue gases. Curr. Environ. Issues Challenges. Springer; 2014. p. 73–111.
[95] Visigalli S, Barberis MG, Turolla A, Canziani R, Berden Zrimec M, Reinhardt R, et al. Electrocoagulation–flotation (ECF) for microalgae harvesting – a review. Sep Purif Technol 2021;271:118684 https://doi.org/10.1016/j.seppur.2021.118684
[96] Vandamme D, Foubert I, Muylaert K. Flocculation as a low-cost method for harvesting microalgae for bulk biomass production. Trends Biotechnol 2013. https://doi.org/10.1016/j.tibtech.2012.12.005
[97] Schenk PM, Thomas-Hall SR, Stephens E, Marx UC, Mussgnug JH, Posten C, et al. Second generation biofuels: high-efficiency microalgae for biodiesel production. Bioenergy Res 2008;1:20–43.
[98] Koh PTL, Andrews JRG, Uhlherr PHT. Modelling shear-flocculation by population balances. Chem Eng Sci 1987;42:353–62. https://doi.org/10.1016/0009-2509(87)85065-0
[99] Sadegh-Vaziri R, Babler MU. PBE modeling of flocculation of microalgae: investigating the overshoot in mean size profiles. Energy Procedia 2017;142:507–12. https://doi.org/10.1016/j.egypro.2017.12.079
[100] Sadegh-Vaziri R, Ludwig K, Sundmacher K, Babler MU. Mechanisms behind overshoots in mean cluster size profiles in aggregation-breakup processes. J Colloid Interface Sci 2018;528:336–48. https://doi.org/10.1016/j.jcis.2018.05.064
[101] Golzarijalal M, Zokaee Ashtiani F, Dabir B. Modeling of microalgal shear-induced flocculation and sedimentation using a coupled CFD-population balance approach. Biotechnol Prog 2018;34:160–74. https://doi.org/10.1002/btpr.2580
[102] Shen X, Toorman EA, Lee BJ, Fettweis M. Biophysical flocculation of suspended particulate matters in Belgian coastal zones. J Hydrol 2018;567:238–52. https://doi.org/10.1016/j.jhydrol.2018.10.028
[103] Kumar S, Ramkrishna D. On the solution of population balance equations by discretization - II. A moving pivot technique. Chem Eng Sci 1996. https://doi.org/10.1016/0009-2509(95)00355-X
[104] Vlieghe M, Coufort-Saudejaud C, Liné A, Frances C. QMOM-based population balance model involving a fractal dimension for the flocculation of latex particles. Chem Eng Sci 2016;155:65–82. https://doi.org/10.1016/J.CES.2016.07.044
[105] Jeldres RI, Fawell PD, Florio BJ. Population balance modelling to describe the particle aggregation process: a review. Powder Technol 2018;326:190–207. https://doi.org/10.1016/j.powtec.2017.12.033
[106] Schmideder S, Kirse C, Hofinger J, Rollié S, Briesen H. Modeling the separation of microorganisms in bioprocesses by flotation. Processes 2018;6:1–22. https://doi.org/10.3390/pr6100184
[107] Smoluchowski M v. Grundriß der Koagulationskinetik kolloider Lösungen. Kolloid-Z 1917;21:98–104. https://doi.org/10.1007/BF01427232
[108] Lee PY, Pahija E, Liang YZ, Yeoh KP, Hui CW. Population balance equation applied to microalgae harvesting. Elsevier Mass SAS 2018;vol. 43. https://doi.org/10.1016/B978-0-444-64235-6.50228-X
[109] Pahija E, Lee PY, Hui C-W, Sin G. Modelling of harvesting techniques for the evaluation of the density of microalgae. Appl Biochem Biotechnol 2022;194:5992–6006.

[110] Lee PY, Yeoh KP, Hui CW. Population balance equation applied to microalgae filtration. Elsevier Mass SAS 2019;vol. 46. https://doi.org/10.1016/B978-0-12-818634-3.50279-4
[111] Ventura SP, Nobre BP, Ertekin F, Hayes M, Garciá-Vaquero M, Vieira F, et al. Extraction of value-added compounds from microalgae. Microalgae-Based Biofuels Bioprod. Elsevier; 2017. p. 461–83. https://doi.org/10.1016/B978-0-08-101023-5.00019-4
[112] Singh M, Ranade V, Shardt O, Matsoukas T. Challenges and opportunities concerning numerical solutions for population balances: a critical review. J Phys A Math Theor 2022;55:383002.
[113] Dürr R, Bück A. Approximate moment methods for population balance equations in particulate and bioengineering processes. Processes 2020. https://doi.org/10.3390/PR8040414
[114] Di Caprio F, Pagnanelli F, Wijffels RH, Van, der Veen D. Quantification of Tetradesmus obliquus (Chlorophyceae) cell size and lipid content heterogeneity at single-cell level. J Phycol 2018;54:187–97. https://doi.org/10.1111/jpy.12610
[115] Kaplan Y, Reich S, Oster E, Maoz S, Levin-Reisman I, Ronin I, et al. Observation of universal ageing dynamics in antibiotic persistence. Nat 2021 6007888 2021;600:290–4. https://doi.org/10.1038/s41586-021-04114-w
[116] Van Heerden JH, Wortel MT, Bruggeman FJ, Heijnen JJ, Bollen YJM, Planqué R, et al. Lost in transition: startup of glycolysis yields subpopulations of nongrowing cells. Science (80-) 2014;343:1245114. https://doi.org/10.1126/science.1245114
[117] Shu C-C, Chatterjee A, Hu W-S, Ramkrishna D. Modeling of gene regulatory processes by population-mediated signaling: new applications of population balances. Chem Eng Sci 2012;70:188–99. https://doi.org/10.1016/j.ces.2011.07.062
[118] Chrysinas P, Kavousanakis ME, Boudouvis AG. Effect of cell heterogeneity on isogenic populations with the synthetic genetic toggle switch network: bifurcation analysis of two-dimensional cell population balance models. Comput Chem Eng 2018;112:27–36. https://doi.org/10.1016/j.compchemeng.2018.01.021